VASCULATURE-ON-CHIP: CHARACTERIZING SHEAR STRESS EFFECTS ON ENDOTHELIAL CELLS

by
ALIREZA TAJEDDIN

Submitted to the Graduate school of Engineering and Natural Sciences
in partial fulfillment of
the requirements for the degree of Master of Science

Sabancı University
July 2022

ABSTRACT

VASCULATURE-ON-CHIP: CHARACTERIZING SHEAR STRESS EFFECTS ON ENDOTHELIAL CELLS

ALIREZA TAJEDDIN

MECHATRONICS ENGINEERING M.Sc. THESIS, MAY 2022

Thesis Supervisor: Assist. Prof. Dr. Nur Mustafaoğlu

It is well known that mechanical stimuli, which have significant effects on cell biology, are the subject of an emerging field of science called mechanobiology. This is accompanied by the development of organ-on-chip as a breakthrough branch of technology and excellent *in vitro* models for the study of organs, diseases, tissue engineering, drug development, and the exploration of the interface between biology and physical forces. Fluid shear stress is one of the essential mechanical forces constantly acting in our vascular system due to blood flow. The endothelial cells lining the interior of the vessel directly sense the shear stress and respond accordingly. Therefore, in order to obtain an accurate organ-on-chip model, which usually includes the vessels on one side, it is essential to apply near-physiological shear stress. This research addresses the design, fabrication, and modification of a microfluidic device to model vessels and characterizes endothelial cell shear. The goal was to approximate *in vivo* shear conditions by setting a constant flow rate and investigating the effects of other parameters. Viscosity, size, and geometry were considered as parameters based on theoretical shear stress expressions. The results support the conclusion that there is a significant morphological response when the viscosity of the flow increases, which was not observed when other parameters were changed. In addition, a novel observation in this field is that endothelial cells function better when the spatial gradient of shear stress is high (viscosity-dominated) than when the temporal gradient of shear stress is high (velocity-dominated).

ÖZET

TEZ BAŞLIĞI

ALIREZA TAJEDDIN

MEKATRONİK MÜHENDİSLİİĞİ YÜKSEK LİSANS TEZİ, MAYIS 2022

Tez Danışmanı: Assist. Prof. Dr. Nur Mustafaoğlu

Anahtar Kelimeler: kayma gerilimi, çip üzerinde damar sistemi, mechnobiyoloji, çip üzerinde organ, endotel hücreleri

Hücre biyolojisi üzerinde önemli etkileri olan mekanik uyaranların, mekanobiyoloji adı verilen yeni bir bilim alanının konusu olduğu iyi bilinmektedir. Buna, çığır açan bir teknoloji dalı olarak organlar, hastalıklar, doku mühendisliği, ilaç geliştirme ve biyoloji ile fiziksel güçler arasındaki arayüzün araştırılması için mükemmel *in vitro* modeller olan çip üzerinde organ teknolojileri eşlik etmektedir. Akışkan kesme gerilimi, kan akışı nedeniyle damar sistemimizde sürekli olarak etki eden temel mekanik kuvvetlerden biridir. Damarın içini kaplayan endotel hücreleri, kesme stresini doğrudan algılar ve buna göre tepki verir. Bu nedenle, genellikle bir taraftaki damarları içeren doğru bir organ çip modeli elde etmek için, fizyolojik bir kayma gerilimine yakın bir kuvvet uygulamak esastır. Bu araştırma, damarları modellemek ve endotel hücre kaymasını karakterize etmek için mikroakışkan bir cihazın tasarımını, üretimini ve modifikasyonunu ele almaktadır. Araştırmanın amacı sabit bir akış hızı ayarlayarak ve diğer parametrelerin etkilerini araştırarak *in vivo* kesme koşullarını yaklaşık olarak tahmin etmektir. Viskozite, boyut ve geometri, teorik kayma gerilimi ifadelerine dayalı parametreler olarak kabul edilmiştir. Sonuçlar, diğer parametreler değiştirildiğinde gözlenmeyen, akışın viskozitesi arttığında önemli bir morfolojik tepki olduğu sonucunu desteklemektedir. Ek olarak, bu alandaki yeni bir gözlem, endotel hücrelerinin, kayma stresinin uzamsal gradyanı yüksek olduğunda (viskozitenin baskın olduğu), kayma stresinin zamansal gradyanının yüksek olduğu (hızın baskın olduğu) duruma göre daha iyi çalıştığıdır.

ACKNOWLEDGEMENTS

Dedicated to those who bring smiles to faces :)

TABLE OF CONTENTS

LIST OF TABLES

LIST OF FIGURES

LIST OF ABBREVIATIONS

KLF: Krüppel-Like Factor

EC: Endothelial cell

ECM: Extracellular Matrix

WSS: Wall shear stress

BBB: Blood-brain barrier

HUVEC: Human umbilical vein endothelial cell

PCR: Polymerase chain reaction

MEMS: Micro-electro-mechanical systems

OOC: Organ-on-chip

PDMS: Poly(dimethylsiloxane)

PECAM-1: Platelet endothelial cell adhesion molecule-1

CD31: Cluster differentiation-31

1. INTRODUCTION

Studying physical forces and mechanical characteristics of cells is known as "Mechanobiology", which is an emerging field of science. It reverts to more than a hundred years ago when a Scottish mathematical biologist named D'Arcy Wentworth Thompson (1860–1948) brought the concept to light by publishing his book, *On Growth and Form* (Thompson & Bonner, 1992). Since then, researchers have aimed to develop it by postulating theorems and integrating concepts from other disciplines to establish a quantitative field of science. The field focuses on identifying the fundamental roles of physical components that cells can sense, including forces, geometry, and matrix elasticity (Lim, Bershadsky & Sheetz, 2010).

At first glance, it seems that cells can only sense biochemical cues. It has been discovered that mechanical stimuli are also determining factors for the function, morphology, and regeneration of cells and tissues that affect human physiology and pathology (Vogel & Sheetz, 2006). Mechanical cues can be categorized into intrinsic and extrinsic. Intrinsic cues deal with single-cell properties like elasticity, stiffness, and viscoelasticity while extrinsic ones are about cell-environment, cell-to-cell, and cell-ECM (extracellular matrix) interactions (Lee, Park & Kim, 2016). The process by which a mechanical cue is translated into cell response and biochemical reactions is termed "Mechanotransduction" (Hill & Meininger, 2012).

Mechanotransduction modulates physical or mechanical stimuli to biochemical cues that produce physiological responses(Zhang & Labouesse, 2012). In biology, forces are in a wide range of magnitudes and length scales; subcellular level (e.g actomyosin motors) or organismal level (e.g gravity)(Vining & Mooney, 2017).

The human body is always experiencing a mechanical force; the vasculature is constantly exposed to cyclic compression/tension and shear stress, which arise from the pulsatile nature of blood flow. Wall shear stress (WSS) is a physical force parallel to the blood flow and is sensed by the inner layer forming the lumen of vessels called endothelial cells (EC). ECs play an essential role in angiogenesis and vascular remodeling by generating different cell growth factors and are highly involved in immune and inflammatory responses. It has been long believed that ECs are only regulated by chemical cues like hormones and cytokines but recently the role of me-

chanical stresses are being proved (Lesman, Rosenfeld, Landau & Levenberg, 2016). They experience direct shear stress caused by blood flow accompanied by continuous pulsatile strain (Price, Wong, Truslow, Leung, Acharya & Tien, 2010). This hemodynamic force is associated with several physiological phenomena including vascular pathologies, morphogenesis, and gene expression means ECs are changing morphology and alter different gene expressions accordingly and might cause different diseases (Souilhol, Serbanovic-Canic, Fragiadaki, Chico, Ridger, Roddie & Evans, 2020). Atherosclerosis and vascular malformation are diseases related to abnormal characteristics of vessels getting signals from fluid shear stress (Baeyens, Bandyopadhyay, Coon, Yun & Schwartz, 2016). There are several studies about the effect of fluid shear stress on EC response including gene expression and also morphology.

The first attempt into understanding the mechanobiology of arterial responses to shear stress was by Rosen et. al. by doing an *in vitro* experiments using cell culture (Rosen, Hollis & Sharma, 1974). They showed that variation in fluid flow in EC produces an enzyme (histidine decarboxylase) that is necessary for the production of histamine. The research followed by Malek and Izumo, they investigated the shape change of ECs when exposed to shear stress. They considered several hypotheses including tyrosine kinase (TK) and ion channels as the dominant mechanism and reported their relation with the cell shape and alignment (Malek & Izumo, 1996). In recent studies, Sonmez et al. conducted research about the cell polarization and orientation to flow in a microfluidic device (Sonmez, Cheng, Watkins, Roman & Davidson, 2020). They reported that the involved mechanisms for sensing the shear are flow dependent, whereas their upstream condition received signals from both physical and biochemical responses to flow. Russo et al. studied the altered shear stress effect on EC and the subsequent response to the extracellular matrix and found it an important concept to fully understand cardiovascular diseases (Russo, Banuth, Nader & Dreyfuss, 2020). They used rabbit endothelial cells and applied biosynthesis analysis and cell-based assays and concluded that vascular biology is directly dependent on mechanical forces. Tsaryk et al. performed a deep study on gene regulation of ECs when exposed to shear stress (Tsaryk et al., 2022). The outcome showed a set of genes that were up- and down-regulated using RNA-Seq and human umbilical vein endothelial cells (HUVEC). KLF4, KLF2 and PI16 are among the upregulated ones, while KIT, ANGPT2, and IRS2 have been downregulated.

Vascular permeability is another critical characteristic that is mediated by fluid shear stress (Partyka, Godsey, Galie, Kosciuk, Acharya, Nagele & Galie, 2017). This is especially important in studying and modeling barrier functions, as it exists in the blood-brain barrier (BBB) (Park, Mustafaoglu, Herland, Hasselkus, Mannix, FitzGerald, Prantil-Baun, Watters, Henry, Benz, Sanchez, McCrea, Goumnerova,

Song, Palecek, Shusta & Ingber, 2019). BBB is a highly selective border made up of brain endothelial cells that has a semipermeable property and prevents solutes in the circulating blood from crossing into the central nervous system (CNS) non-selectively (Lee, Chung, Lee & Jeon, 2020). To interrogate the effects of fluid shear stress on permeability and tight junction proteins, DeOre et al. proposed an *in vitro* model to study BBB. They applied transendothelial electrical resistance (TEER) measurement and also other assays like immunocytochemistry, dextran permeability, and gene monitoring and concluded that a minimum amount (threshold) of shear stress is necessary to observe barrier function (DeOre, Partyka, Fan & Galie, 2022). Furthermore, organ-on-chips mostly consist of one side recapitulating vasculature. Examples are usual single organ models like BBB-on-chip (Wevers, Kasi, Gray, Wilschut, Smith, van Vught, Shimizu, Sano, Kanda, Marsh & others, 2018), Lung-on-chip (Benam, Villenave, Lucchesi, Varone, Hubeau, Lee, Alves, Salmon, Ferrante, Weaver & others, 2016), liver-on-chip (Kim, Lee, Kim, Ro, Kim, Min, Park, Sunkara, Park, Michael & others, 2020), and gut-on-chip (Ashammakhi, Nasiri, De Barros, Tebon, Thakor, Goudie, Shamloo, Martin & Khademhosseini, 2020). So, it is important to mimic real physiological conditions for the purpose of more reliable results. Also, there are some chips specifically designed just to study vasculature (vasculature-on-chip). Recently, Lu et al. employed a vasculature-on-chip platform to study SARS-CoV-2 infection on endothelial cells (Lu, Lai, Rafatian, Gustafson, Campbell, Banerjee, Kozak, Mossman, Mubareka, Howe & others, 2022). They modeled infection of the virus alone and also the interaction of the infected cells on the permeability. They reported that viruses reduced barrier function (VE-cadherin) and also had an effect on inflammatory cytokines. Also, in another study, Kim et al. developed a microfluidic device to study the cellular programs during normal angiogenesis by co-culturing endothelial cells with fibroblast cells (Kim, Lee, Chung & Jeon, 2013). They showed the morphological and biochemical characteristics of *in vivo* blood cells and exhibit barrier function and stability.

Therefore, shear stress is an indispensable part of organ-on-chip models considering its role in mediating and regulating biological phenomena. There are many attempts to recapitulate the vasculature by employing organ-on-chips. The main research interests are angiogenesis and vasculature which greatly enjoy organ-on-chips since it manipulates physics, chemistry, and biology at an exact scale (Haase & Kamm, 2017). To get a near-physiological environment and apply real shear stress of organs, the main concern is that it requires high flow rates, which affects the studies inversely mainly for two reasons; i) cells will be washed by the high-momentum flow, ii) consuming a high amount of cell culture media in long term culture. In this study, we proposed a new *in vitro* model to study and characterize shear stress in vasculature. The first and main question of the research is how to apply higher

3

shear stress on ECs with a constant flow rate?

The model can apply a set of controlled parameters on ECs that are directly related to shear stress. These parameters are viscosity, dimension, and curvature. This report is about the design, fabrication, modification, and testing of a vasculature chip model. The conceptual design has been developed according to arterioles specifications and also modeled numerically. The fabrication of microfluidic devices is explained thoroughly followed by how the surface has been characterized and modified. This was mentioned as the second question of the research stating which combination of coatings can provide a suitable ECM for cells and at the same time capable for long-term cultures? Indeed, it was a prerequisite practice before addressing the main question. The design of experiments (DOE) has been performed according to the real size of the vessels (arterioles), the actual blood viscosity, and also the curvature nature of vasculature. Cell responses have been visualized by staining and an automatic cell segmentation and shape analysis has been used to process the images.

The following sections explain the details about the shear stress effect on cells, microfluidic devices and organ-on-chips, mechanical stimuli in chip models, the conceptual design, and fabrication. In addition, data about characterization and modification of the chip are provided both experimentally and numerically. Finally, the cell experiment and analysis are presented and covered by a discussion.

2.   THEORY

This chapter introduces the interface between biology and physics, where mechanical forces induce biological responses. The concept of mechanobiology and related terms are discussed thoroughly. The emphasis will be on shear stress and how this force is regulating and affecting cell biology.

2.1 What is Mechanobiology?

Mechanobiology can be involved in every aspect of cell biology in which any mechanical force is generated, transmitted, or sensed and result in an alternation in cell function (Humphrey & Schwartz, 2021). Cell function is the primary focus of cell biology since cells are the smallest and microscopic units of life. Researchers also try to understand the effect of physiological environment, cell structure, and interactions with extracellular matrix on cell function to investigate diseases and help the biomedical field (Bosman & Stamenkovic, 2003). Later, the analytical concept of biochemistry improves understanding of the field, including various cellular processes and pathologies (Harris & Korolchuk, 2019). Now it can be stated that mechanobiology is connecting cell biology and biochemistry with concepts in mechanics including solid, fluid, viscoelasticity, and experimental or computational mechanics.

Cell function is well regulated *in vivo* when all requirements for biological and mechanical signals arising from neighboring cells and the extracellular matrix (ECM) are integrated with each other. Hence, it is an ultimate goal of mechanobiology as the lost chain of this system to give a more comprehensive vision about the physiology which is helpful for improving the available knowledge and models and indeed different for each organ. (Wang & Thampatty, 2006).

Arterial mechanobiology varies at different sites with branch points and curved re-

gions that cause changes in the flow pattern and induced forces. Furthermore, the arterial system often adapts to the altered mechanical load by the cell and extracellular matrix in the development of complex configurations (Humphrey, 2008). The arterial system also shows a remarkable ability to adapt to responses to disease, injury, and clinical treatment.

2.1.1 Mechanotransduction

Mechanotransduction is a biological concept in which mechanical forces applied to cells turn into (transduce into) biochemical signals and result in cell responses, vascular tone control, and homeostasis. This sensing is achieved by several endothelial cell elements some of which are proven and others are under investigation by different research groups. However, the potential mechanosensory systems on the cells can be listed as cytoplasmic receptors, ion channels, kinases, integrins, G proteins, PECAM-1, and ECM. Figure 2.1 illustrates some of the important mechanisms for sensing physical signals in EC.
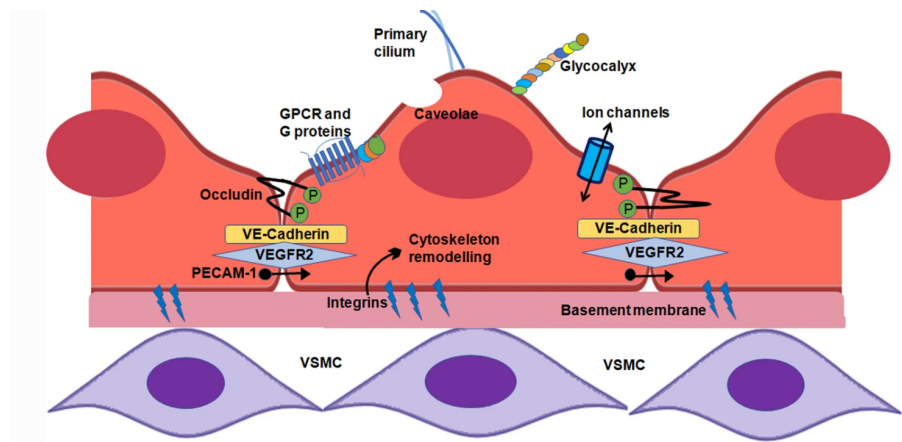
Figure 2.1 Important mechanosensors in vasculature EC. Figure from (Karthika et al., 2021)

Integrins are known as a family of transmembrane heterodimers (more than 20 types) that are composed of subunits α and β. The domains in the extracellular part bind with specific ECM ligands like fibronectin, vitronectin, and collagen types. The other part (cytoplasmic) interacts with the focal adhesion sites(Sastry & Horwitz, 1993). The specific binding to ECM ligands triggers the activation of signals in the presence of external forces as well as shear stress (Schwartz, Schaller & Ginsberg, 1995).

6

Ion channels are another sensing mechanism activated by shear stress. Studies have shown that shear stress increases the permeability of the cell membrane to K^+ (Alevriadou, Eskin, McIntire & Schilling, 1993). Also, shear stress improves the influx of Ca^{2+} in ECs which results in cellular signaling regulation. This is a rapid response as the concentration of Ca^{2+} enhances significantly even by 1 minute of shear stress exposure (Ando, Komatsuda & Kamiya, 1988).

PECAM-1 also known as cluster differentiation-31 (CD31) is a glycoprotein with a molecular mass of 130 kDa that is expressed in ECs, platelets, and leukocytes and has an essential role in leukocyte aggregation. It is also located at junction sites between the ECs when there is a confluent monolayer. Shear stress induces changes in EC junctions that are expressed by PECAM-1 (Osawa, Masuda, Kusano & Fujiwara, 2002).

G Proteins are another fast-activated mechanism after the onset of shear stress (in 1 second). G protein-coupled receptors (GPCRs) are the main classes of receptors on the cell surface (Morris & Malbon, 1999).

2.2 Different forces experienced by cells

Two main categories of forces are being applied to the cell; i) external and ii) internal forces. Forces that are arising from the cell environment are external like tensile, compressive, and shear stresses. Depending on the organ and the cell types, it can also be a combination of these forces. ECs that form the inside surface of human vessels experience tensile stress, hydrostatic pressure, and fluid shear stress. The internal forces are those generated by cells and are called intercellular tension. These forces are regulated by cross-bridging of actomyosin and transferred to ECM referred to as cell traction forces.
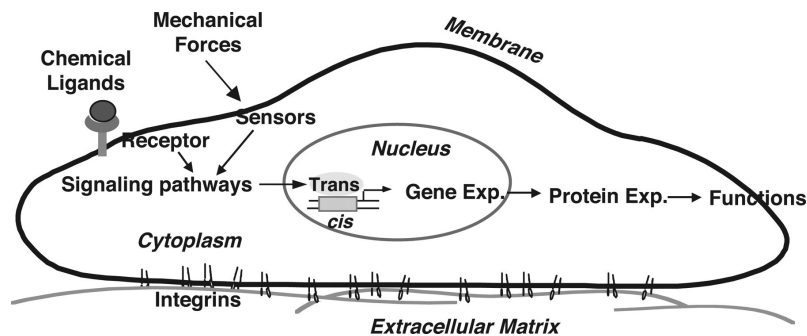
Figure 2.2 forces acting on cells. Figure from (Chien, 2007)

2.3 Shear Stress effect

Considerable shreds of evidence support the fact that CE growth depends on the type of shear stress that they are experiencing. These effects are recorded for cell function, signaling pathways, and gene expressions. Previous studies demonstrate that shear stress in low Reynolds numbers (laminar) causes a reduction in the proliferation rate of ECs (Levesque, Nerem & Sprague, 1990). Also, in another research, the effect of long-term exposure to high shear stress on the rate of DNA synthesis has been evaluated which showed a lower rate compared to a static condition (Mitsumata, 1991). Further studies are aimed at investigating the flow pattern, particularly in disturbed flows, and its effect on ECs (Chien, 2008). New flow pattern studies concluded that pulsatile flow with a considerable forward flow reduces the EC proliferation but a reciprocal oscillatory flow (no direction) has a positive effect as the disturbed flow does (Li, Haga & Chien, 2005).

Proven results also show that shear stress affects EC signaling pathways. It is occurring by activating multiple signaling molecules such as protein kinase C (PKC) and P13K which result in initiating mechano-sensing mechanisms mentioned in Section 2.1.1. and propagation of signals (Kuchan & Frangos, 1993).

Gene expression assays such as RT-PCR have shown that EC exposed to flow inside channels have a gene expression record due to shear (Chien, Li & Shyy, 1998). A recent study on ECs and shear expression found that the expression of transcription factors KLF2 and KLF4 which are known as master regulators of EC shear stress response have been upregulated. This up-regulation occurs 30 min after inducing shear stress on ECs (Tsaryk et al., 2022). Figure 2.3 shows some up and down-regulated gene expressions due to shear stress in HUVEC cells.
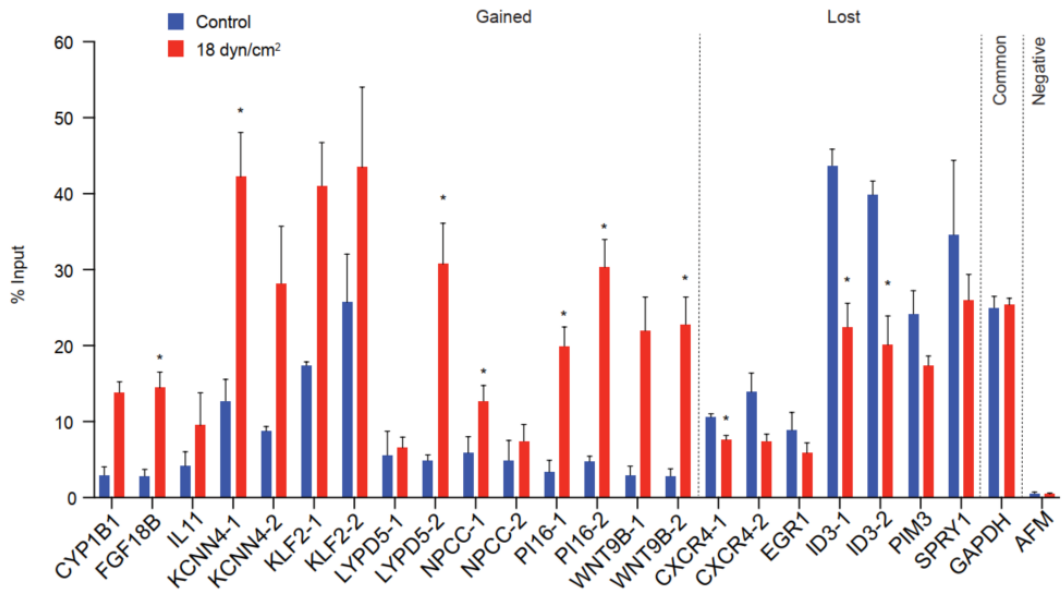
Figure 2.3 HUVEC exposed to shear stress for 30 min. Figure from (Tsaryk et al., 2022)

2.3.1 Hemodynamics & blood flow

Hemodynamics is the physical study of blood flow considering all solid structures (e.g. arteries) through which it flows (Secomb, 2016). Blood is classified as a non-Newtonian fluid and as a suspension containing 45% cellular components by volume. The suspending medium is called plasma and contains of proteins and electrolytes showing Newtonian behaviors in terms of viscous properties. The cellular components are red blood cells, several types of white blood cells, and platelets. Red blood cells are the dominant contributor to the viscosity of the blood, which varies by the volume fraction of red blood cells called hematocrit.

Blood is a shear-thinning fluid; blood viscosity increases by a decrease in shear rate. Furthermore, it depends on the flow rate and the diameter of the vessel (Humphrey & Delange, 2004). Figure 2.4 demonstrates the shear stress vs. shear rate curve of a shear-thinning fluid where the slope of the graph is the viscosity. Two main reasons for this non-Newtonian behavior can be presented; at low-velocity gradients (shear rate), red blood cells aggregate and it increases the blood viscosity. At higher velocities and also lower dimensions (with a threshold of 5-7μm) these aggregations will break down and the cells will also deform to have less resistance to the inner surface of the vessel (Chien, 1975).
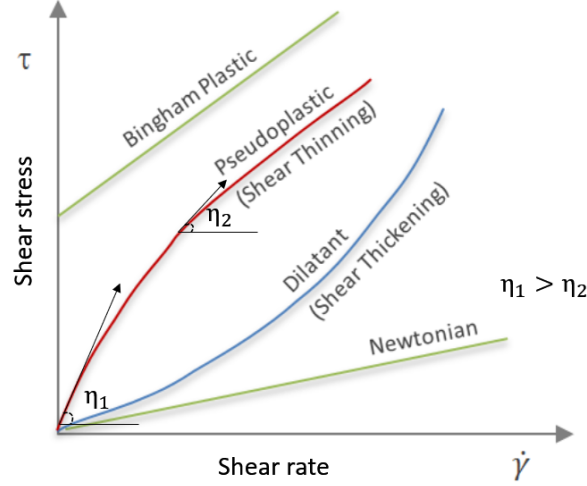
Figure 2.4 Shear stress vs shear rate in a shear-thinning fluid. Figure from (Polymerdatabase, Polymerdatabase)

According to the Interacting Continua theory (Mixture theory), blood is modeled as a two-component mixture which is plasma and red blood cells (Kim, Antaki & Massoudi, 2016). In this regard, there are attempts to present expressions of blood viscosity in terms of dimensions and hematocrit. Pries et al. performed a comprehensive analysis of the experimental data to find a description of apparent viscosity as a function of vessel diameter and hematocrit. The outcome is an empirical equation to describe the relative viscosity (μ_{rel}) (the ratio of apparent viscosity to suspension medium viscosity) (Pries, Neuhaus & Gaehtgens, 1992):

$$\mu_{rel} = 1 + (\mu_{0.45} - 1) \frac{(1 - H_D)^C - 1}{(1 - 0.45)^C - 1} \tag{2.1}$$

Where

$$\mu_{0.45} = 220 exp(-1.3D) + 3.2 - 2.44 exp(-0.06^{0.645}) \tag{2.2}$$

D is the diameter in μm. H_D in equation (2.1) is called discharge hematocrit and is defined as the volume flow rate of red blood cells at a fraction of the total volume flow rate. There is a relation between tube hematocrit (H_T) and discharge hematocrit (H_D) based on the Fåhraeus effect.

The Fåhraeus effect is caused by the particulate and non-continuum nature of the blood. There are regions near the walls which form cell-free or cell-depleted regions. Due to the flexibility of red blood cells, under the condition of increased aggregation, they migrate to the core of the vessel and the resistance in the slow-moving parts near walls (non-slip wall condition) will decrease. Therefore, there is a difference in the volume concentration of blood cells inside the tube and when they enter or

10

leave the tube. They proposed an expression that can be used for (2.1):

$$\frac{H_T}{H_D} = H_D + (1 - H_D)(1 + 1.7e^{-0.35D} - 0.6e^{-0.01D}) \tag{2.3}$$

To find H_D, we can substitute the normal hematocrit in the body which is 38.3 to 48.6% for men; and 35.5 to 44.9% for women which are also presented in table 2.1 (Walker, Hall & Hurst, 1990). Finally, the term C in equation (2.1) relates the viscosity to hematocrit as per the following equation:

$$C = (0.8 + exp(-0.075D))(-1 + (1 + 10^{-11}D^{12})^{-1}) + (1 + 10^{-11}D^{12})^{-1} \tag{2.4}$$

Table 2.1 Hematocrit range in human

	$H_T\%$
Women	35.5-44.9
Men	38.3-48.6
Average	41.83 ±2.99

Therefore, considering the average hematocrit for men and women shown in table 2.1 and plugging it into equation (2.3), the discharge hematocrit can be found for different diameters. Figure 2.5-A shows the plot of equation (2.1) with the described parameters; the graphs are for three different amounts of discharge hematocrit including the reference value (45%), the average (41.8%) and the minimum (15%) to compare with the experimental data. There is a good agreement with the experimental data provided by Pries et al. (Pries et al., 1992) as shown in Fig.2.5-B.
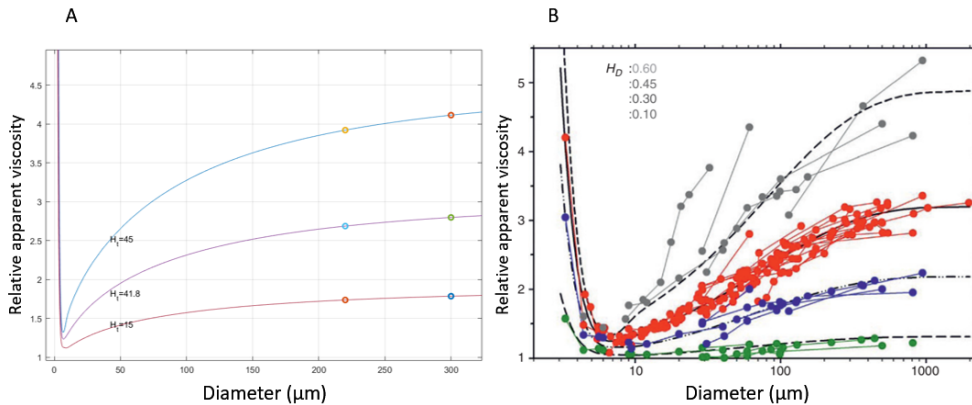
Figure 2.5 Relative apparent viscosity versus diameter for different H_D

2.4 Microfluidics

This section discusses the importance of using microfluidic devices and how near-physiological *in-vitro* environments can be modeled by them. It has been followed by design concepts and considerations.

2.4.1 Microfluidic devices

Due to the recent progress in the field of miniaturization, it is almost possible to scale down any system like mechanical, fluidics, or electromechanical. The attempt started with the well-known field of MEMS (micro-electro-mechanical systems) in the 1990s and branched into other disciplines including chemical, biological and biomedical. Sometimes, there were fluid flows under new physical conditions and unexplored, which required the concept of microfluidic devices. Microfluidics can be defined as the study of fluid flows with different conditions (laminar/turbulent, single/multiphase) working in a microsystem. Microfluidic devices are the tools for this study.

There are advantages offered by microfluidic devices and specifically organ-on-chips which are significant drivers for their rapid development in the recent decades(Fiorini & Chiu, 2005). Precise functioning, low volumes of samples, and the provision of a 3D cell culture platform are mentioned as the beneficial aspect of using organ-on-chips(Chan, Huang, Guo, Ding, Kapur, Mai, Yuen & Huang, 2013).

2.4.2 Organ-on-Chips

Organ-on-chips(OOC) can be defined as biocompatible microfluidic devices that mimic human physiological environments. This is achieved by 3D culturing human cells and controlling external mechanical parameters to accurately recapitulate both cellular structure and essential functions of an organ (Ramadan & Zourob, 2020). Different organs are being investigated by OOCs, including lung, brain, liver, intestine, etc. (Tajeddin & Mustafaoglu, 2021). This technology has enabled enormous

breakthroughs for studying cell biology, disease physiology, and drug development while providing privileged features to available animal models prone to failures in correctly predicting clinical outcomes (Ma, Peng, Li & Chen, 2021).OOC technologies provide promising results for overcoming the shortcomings of drug development models that are highly dependent on costs and timing. Current preclinical testing mainly uses laboratory animals and faces two main problems; (i) the ethical prohibition and (ii) the different responses to the drugs compared to those of human cells. Many preclinical animal tests lead to failures at the final stage of in vivo testing, resulting in a loss of resources and time. Clearly, microfluidic OOC technologies can be one of the key players in solving this problem, as they can serve as platforms for the precise screening of drugs in *in vitro* models based on human cells, leading to more effective results in both the treatment and the reduction in side effects (Ingber, 2020).

2.4.3 Scaling law

The scaling laws can be defined as proportionality relations that exist between any parameters that relate a system to its length scale (Wautelet, 2001). In another word, it is the law of the variation of physical quantities with the size l of the system. As a tangible and familiar example, the volume and surface area of an object is associated with l^3 and l^2, respectively. Thus, we can conclude that the ratio of surface area to volume is larger in smaller objects. Scaling laws can be viewed from two distinct points of view; first, the scaling of the physical size of objects, and the other one is dealing with phenomenological behaviors.

In the process of designing, it is always important to note whether all elements of design are on a similar scale "isomorphic/isometric" or they are performing on different scales ("allometric"). The down- or up-scaling of the systems would result in neglect of the predominant phenomena. When the systems are scaled down and the microscopic scales are reached, the weight of the object will become an insignificant parameter (scaling with l^3), and therefore body forces can be neglected. This is while surface tension becomes predominant (scaling with l). Table 2.2 shows the length scale dependencies for different parameters.

A precise model is extremely dependent on choosing the right scale to have correct physics and not to lose the affective phenomena. For instance, to model fluids in micro scale as are existed in blood capilaries, microfluidic devices are a great tool.

Table 2.2 Parameters and scaling law

Parameter	Scale	Parameter	Scale
Length (L)	L^1	Area (A)	L^2
Volume (V)	L^3	Surface area/Volume (A/V)	L^1
Mass (M)	L^3	Inertial Force (F)	L^3
Stress (σ)	L^1	Surface tension	L^1

As Table 2.2 shows, on microscales, when dimensions (L) approach small values, body forces are negligible and surface tension and shears are the dominant parameters affecting the physics of the model.

2.4.4 Microhydrodynamics

Knowing the pattern and specification of the flow is a prerequisite for analyzing it. It shows which terms of the governing equations are significant to consider. In microsystems that work with Newtonian fluids and the Reynolds number ($Re = \frac{\rho U l}{\mu}$) is low($Re < 1$), the flow is governed by the Stokes equation:

$$\rho F_i - \frac{\delta P}{\delta x_i} + \mu \frac{\delta^2 u_i}{\delta x_j^2} = 0 \tag{2.5}$$

Where, u_i is the velocity component in the i axis, P is the pressure, and F_i is the ith component of external volumetric forces. This equation has beneficial properties in the absence of inertial and body forces that can be listed as linearity, uniqueness of solution, reciprocity, and reversibility.

2.4.5 Shear in micro-scale

As elaborated above, shear stress is one of the fundamental phenomena when the model is scaled down to micrometers. To analyze the flow and obtain the forces on them, we can consider a cubic element in the channel with a square cross-sectional area as illustrated in the figure 2.6.

14
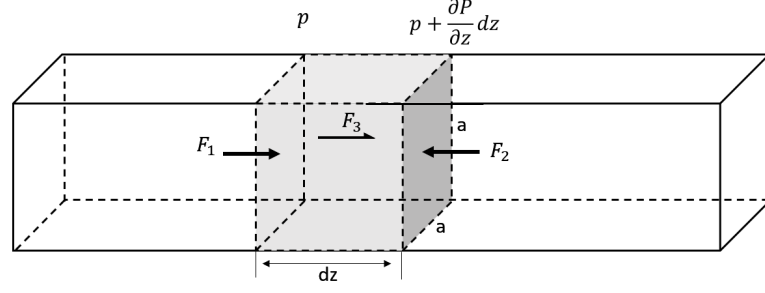
Figure 2.6 Forces acting on a fluid element in a microchannel

At steady state condition, the sum of all involved forces are zero:

$$\Sigma F = F_1 + F_2 + F_3 \tag{2.6}$$

Where F_1 and F_2 are hydrostatic forces ($F_1 = Pa^2$ & $F_2 = -(P + (\frac{\delta P}{\delta z}dz))a^2$). The pressure gradient shows the change along the length of the channel. F_3 is the drag force on the wall surface that can be expressed as:

$$F_3 = surface\ area \times wall\ shear\ stress = \frac{\pi}{4}a^2 dz\tau_w = \pi r_h^2 dz\tau_w \tag{2.7}$$

In equation (2.7) in order to make it analogous with the literature hydraulic radius of the cross-sectional area has been employed.($r_h = \frac{4A}{2P} = \frac{4a^2}{8a} = \frac{a}{2}$) has been used. By substituting the forces inside equation (2.6), we have:

$$\tau_w = \frac{r_h}{2}(\frac{\delta P}{\delta z}) \tag{2.8}$$

It has been proved experimentally that the pressure gradient ($\delta P/\delta z$) is not dependent on the position. Therefore, if the total pressure change (pressure drop) throughout the channel with a length of L is ΔP then:

$$\tau_w = \frac{r_h}{2}(\frac{\Delta P}{L}) \tag{2.9}$$

for Newtonian fluids, the relation between ΔP and Q (flow rate) is obtained using the Hagen-Poieuille relation:

$$\frac{r_h \Delta P}{2L} = \mu(\frac{4Q}{\pi r_h^3}) \tag{2.10}$$

By combining equation (2.10) and (2.9) we can conclude that:

$$\tau_w = \mu(\frac{4Q}{\pi r_h^3}) = \mu(\frac{32Q}{\pi a^3}) \tag{2.11}$$

15

It is worth mentioning that there is a similar expression for shear stress in the pertinent literature as per the following.

$$\tau_w = \mu(\frac{6Q}{wh^3}) \tag{2.12}$$

Here w and h are the width and height of the channel, respectively. Equation (2.12) is only valid for the zero ratio $\frac{h}{w}$ ($w >> h$)(Howell, Jr., Mott, Fertig, Kaplan, Golden, Oran & Ligler, 2005).

2.4.6 Applying Mechanical Stimulus

Cells are experiencing a set of biomechanical and biochemical stimuli that result in a specific cellular response. Biomechanical cues usually have an external nature (extrinsic) and can be categorized as passive or active. As illustrated in figure 2.7, passive biomechanical cues substrate stiffness, and geometrical or topographical confinement are considered during the design and fabrication of the device. While active stimuli are tension/compression, fluid shear stress, interstitial flow, and hydrostatic pressure can still be modulated during the experiments. Shear stress is a common mechanical cue in organ-on-chips since flow is an inseparable part of cell culturing inside microfluidic devices (Young & Beebe, 2010). Therefore, it must be studied and characterized precisely to provide near-physiological conditions for cells.
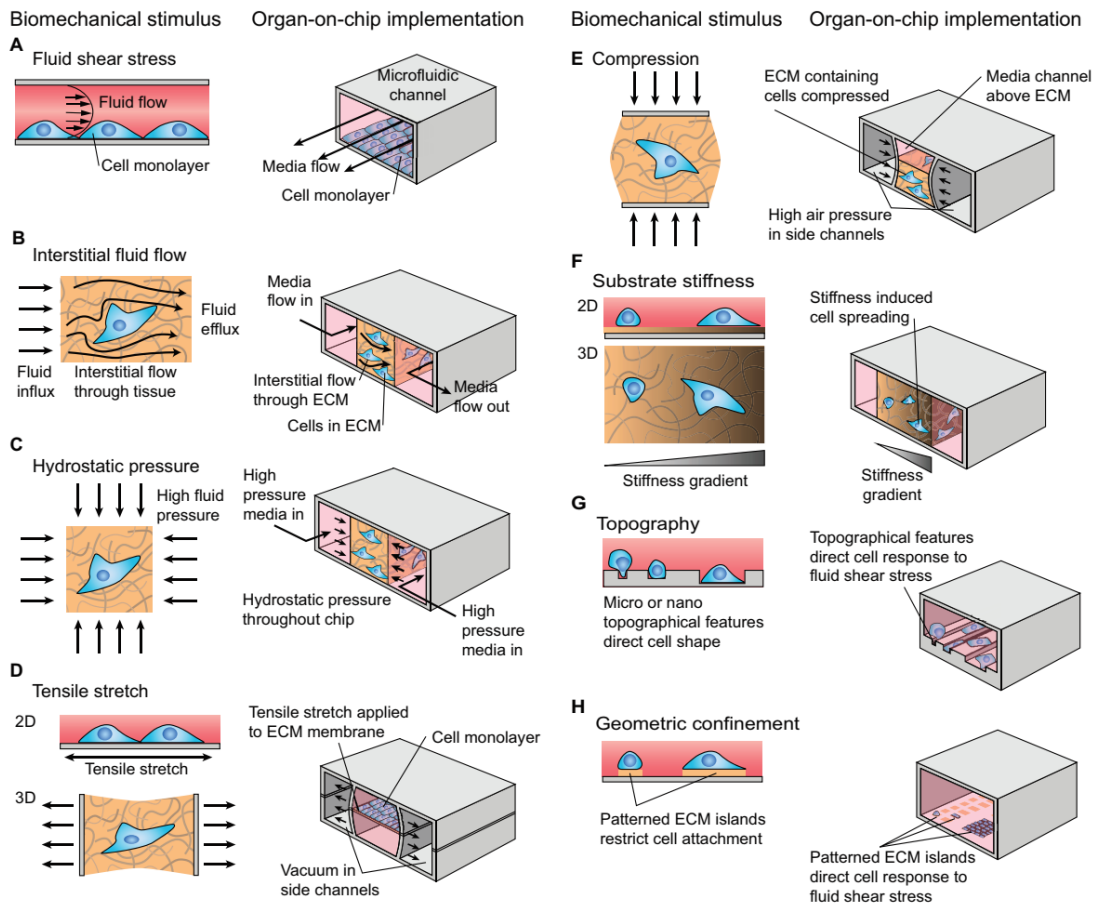
Figure 2.7 Biomechanical cues and their model on organ-on-chips. Figure from the reference (Thompson et al., 2020)

3.   METHODS

This chapter introduced concepts, theories, and methods which have been employed in research. It covers the design and fabrication part, as well as the biological experiments conducted to study the shear effect on the vasculature.

3.1 Design

Designing a microfluidic device to mimic the physiological environment of a functional unit of an organ (here the vasculature) is a combination of physiological and mechanical concepts which are always regulated by material and fabrication thresholds. Definitely, the aim of the design can not be to model the whole features of an organ, but only crucial functions according to the aim of the study.

3.1.1 Conceptual design

There are specific concepts that must be considered during the design of a vasculature environment. In this research, the aim of the study is to investigate the shear effect that is correlated with dimension, viscosity and flow rate (velocity gradient) as elaborated in Section 3.2.2. Equation (3.1) is the final expression of shear in our channels.

$$\tau = \frac{32\mu Q}{\pi a^3} \tag{3.1}$$

Geometry and dimensions: Microfluidic chips are different in terms of dimensions and geometry and are decided in concert with the organ targeted to be studied. The

arterial system is responsible for supplying oxygen to the organ (exceptions are the pulmonary arteries from the heart to the lungs and the umbilical artery). Arterioles are the type between the arteries and the capillaries where oxygen exchange is taking place as shown in figure 3.1.
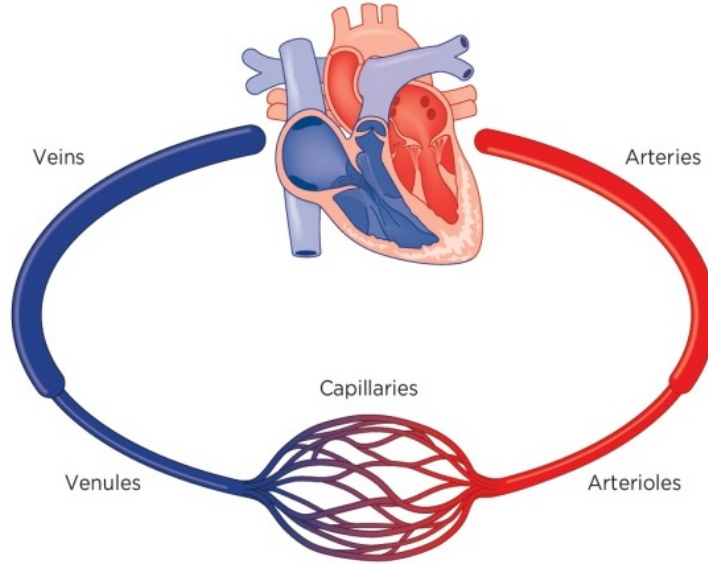
Figure 3.1 Five types of blood vessel

Generally, arteries are classified into elastic, muscular, and arteriole (Bauer, Busse & Schabert, 1982). The elastic arteries have the largest dimensions with a diameter of 1 to 2.5 cm. They are usually not resistant to flow because they have a fairly large lumen, and velocity gradients are imposing considerable changes. Muscular arteries are smaller in diameter compared to elastic types (0.3 mm-1 cm) and function to deliver blood to different organs. Arterioles are the smallest arteries in the body with a dimension range of 0.01-0.3 mm ($10 - 300\mu m$)(Javris, 2018). Thus, the size of our microfluidic channels is in this range.

To have a near real condition of the organ, geometry is also a vital parameter. Most microfluidic channels have been designed as straight channels (Vasant, Appasaheb, Bhausaheb & Sitaram, 2021), However, straight sections of the human vasculature are limited and definitely do not include capillaries. How a cell responds to curvature and shear stress becomes an important question since junctional networks are defined by endothelial cell morphology. For example, in the case of brain vasculature, considering a fixed projected cell area and vessel diameter, cell elongation increases the number of cells around the perimeter and results in an increase in the total length of cell-cell junctions per unit length of the vessel.

Serpentine geometries help to study the effect of vasculature curvature on flow and shear. Dean number is an important parameter in curved flows. As equation (3.2) is showing it is directly dependent on the Reynolds number. Low diameters and

radius of curvature are enhancing dean effects, as well as vortices (Ahmadi, Butun, Altay, Bazaz, Alijani, Celik, Warkiani & Koşar, 2021).

$$De = \frac{\sqrt{\frac{1}{2}(inertial\,forces)(centrifugal\,forces)}}{viscous\,forces} = \sqrt{\frac{d}{2r}}\frac{\rho v d}{\mu} = \sqrt{\frac{d}{2r}}Re \qquad (3.2)$$

Where d is the diameter and r is the radius of curvature. In this research, two different geometries were considered; i) straight and ii) serpentine to compare and study the effect of geometry (Figure 3.2). All the chips are single channels without any membrane.
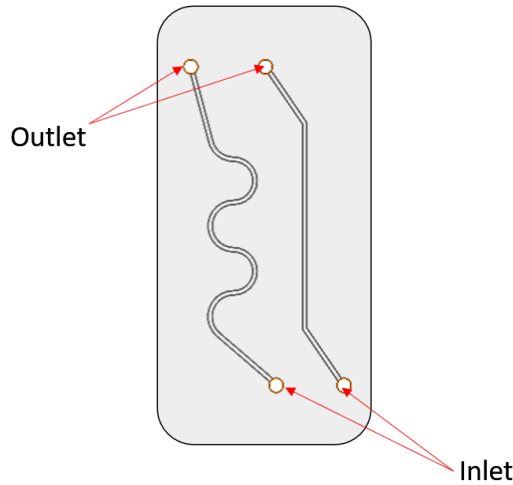
Figure 3.2 Schematic of straight and serpentine micro-channels

Another concept in the design is *clog avoidance*. Working with soft materials on microscales may result in channel clogging (Dersoir, de Saint Vincent, Abkarian & Tabuteau, 2015). This issue can interrupt cell growth and inversely affect the performance of the vasculature chip model.

Generally, clogging occurs through three different mechanisms; (A) sieving, (B) bridging, and (C) aggregation as shown in Figure 3.3.
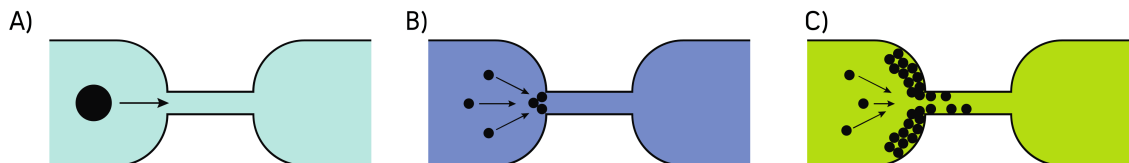
Figure 3.3 Different mechanisms of clogging

Sieving might occur if the size of the particles is larger than the channels which, in the case of soft materials such as cells, will not include the total size due to flexibility.

Bridging is another mechanism that, unlike sieving, small particles are the cause. They form an arch shape along the width of the channels due to the steric effect (spatial arrangement of particles).

Clogging by aggregation is a common mechanism that happens by the deposition of particles. The aggregated layer starts growing due to the hydrodynamic, diffusive, and colloidal effects (Dressaire & Sauret, 2017). In the organ chip models, particles might be dead cells and ECM parts washed by the flow.

In steady low inertia flow, there is a higher probability for particles to clog the channel and remain clogged. Flow oscillation can postpone or remove the onset of clogs by changing the orientation of the particles (Dincau, Dressaire & Sauret, 2020). So, rather than size, flow control and the use of peristaltic pumps are very helpful which has been considered in this study as well.

3.2 Fabrication

Microfabrication is an attempt to miniaturize physical models and devices that include a set of practices different from conventional common manufacturing. There are specific techniques to add, remove, and pattern materials, which all occur on a specific substrate. Generally, organ-on-chips are fabricated through two different approaches: (i) top-down and (ii) bottom-up.

In order to make a bottom-up vasculature-on-chip, the microstructures are defined, and then cells are seeded and will develop their vascular network quiet without any control over them. This is while in the top-bottom approach for fabricating a vasculature, microvessels (microchannels) are defined, and then cells are inserted into the completely defined and controlled scaffolds. The combination of the above is also possible. Here, the top-bottom approach is applied to have control over the dimensions of microvessels.

There are different microfabrication methods to make a microchannel (figure 3.4). The following contains a short description of soft lithography and 3D printing which have been tried in this research a detailed explanation of why we chose 3D printed molds for this fabrication.

Soft lithography: It is a common method based on the popular method of photolithography and is applicable to many materials, particularly elastomers (e.g PDMS)(Qin, Xia & Whitesides, 2010). Fast prototyping and low cost can be mentioned as the two beneficial points of this method. There are the main steps in

terms of microfabrication in this approach:

1- Photoresist coating 2- UV exposure through photomask 3- Applying developer 4- PDMS molding 5- Bonding (Whitesides, Ostuni, Takayama, Jiang, Ingber & others, 2001)

3D printing: Three-dimensional material printing is a new technology to create 3D components and devices even at microscales. It is categorized as additive manufacturing with a layer-by-layer approach in which materials are placed from the bottom to the top. Accompanied by this, nowadays the technology is capable of printing tissues using a combination of cells, matrices, and biomaterials called bioprinting(Aljohani, Ullah, Zhang & Yang, 2018).
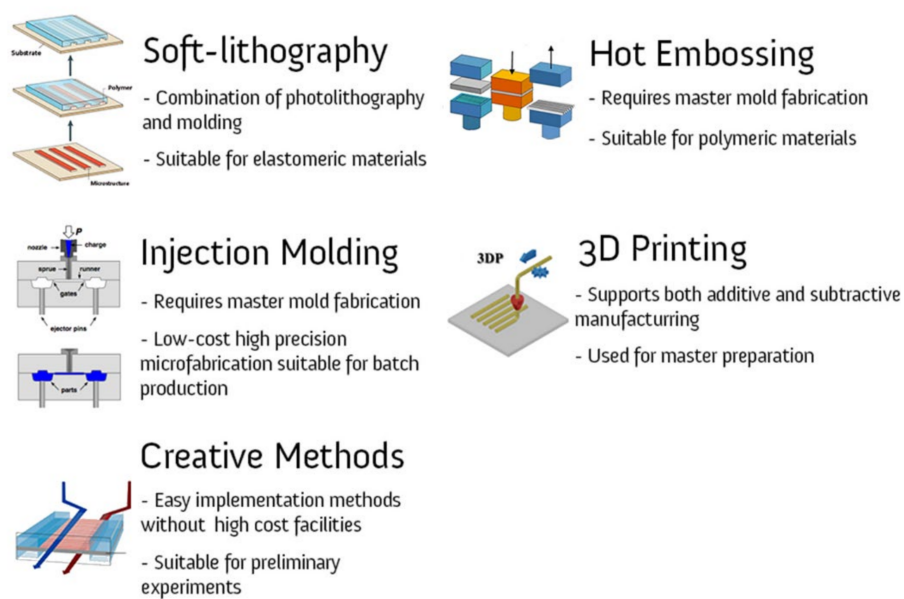
Figure 3.4 Microfabrication methods for organ-on-chips

3.2.1 Mold preparation

The master used in soft lithography can be made either by photolithography or 3D printing. There are advantages and disadvantages that have been summarized in Table 3.1. Both methods require specific facilities and equipment (clean room & high precision 3D printers respectively) so has not been included in the comparison.

So as to have precise square cross-sections for channels, the 3D printer approach

Table 3.1 Photolithography vs. 3D print

Method	Photolithography	3D print
Advantage	- Precision down to 50 μm - High-quality surface	- Fast prototyping - Good control over the height of the channel
Disadvantage	- Contains several steps - Hard to maintain the channel height	- Limited to the printing technology (50 μm) - Higher surface roughness

has been chosen. This is while spin coating a specific thickness of the photoresist (usually negative photoresist) is difficult to achieve as there are limitations according to available data sheets. Figure 3.5 shows the spin speed vs. thickness of SU8-3000 photoresist, which is very common in the field. Achieving thickness beyond 100 μm requires multiple coating which is very demanding.
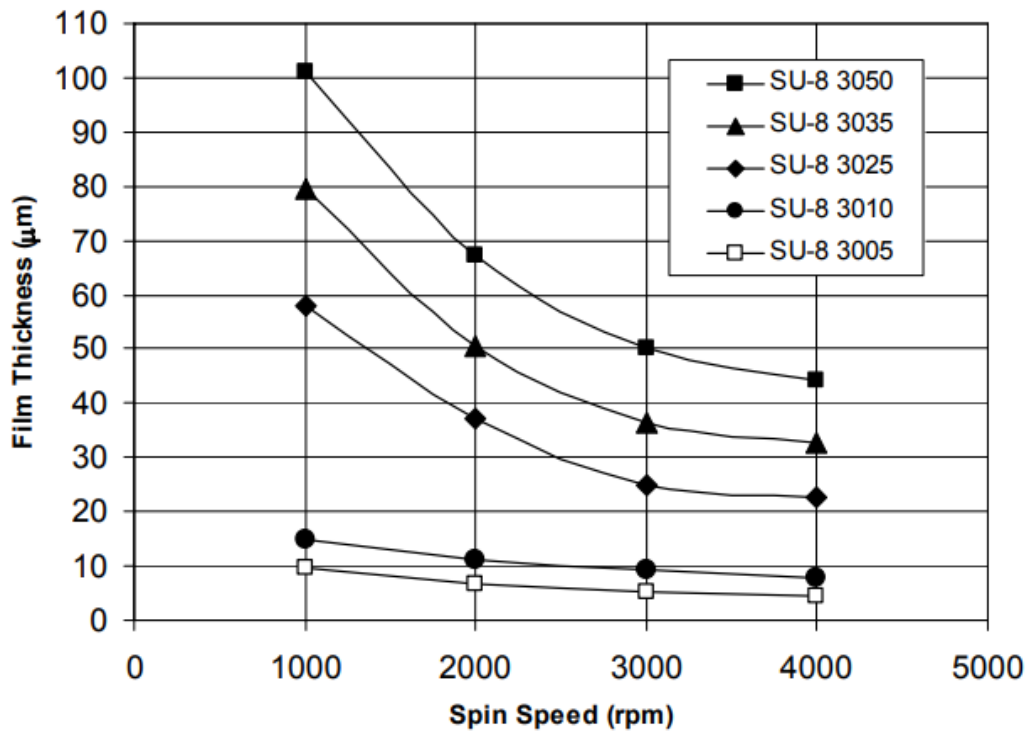
Figure 3.5 Spin speed vs. thickness (SU8-3000)

Therefore, the molds (masters) to follow soft lithography have been made by 3D printing. The design was done in Solidworks software (Figure 3.6) and the appropriate format has been sent for 3D printing (Appendix-A).
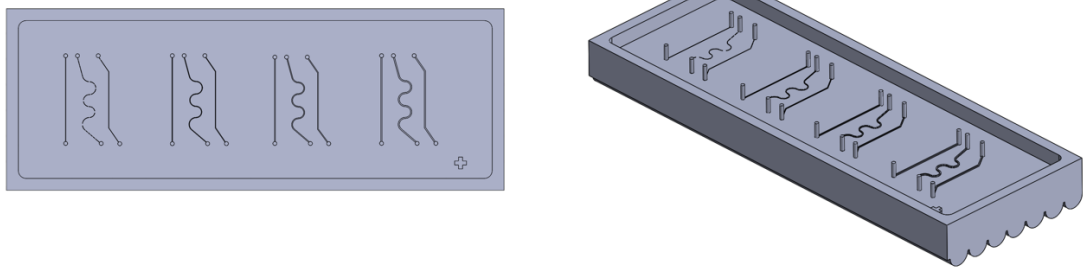
Figure 3.6 CAD design of molds

The molds have been printed with a high precision resin and cured with heat and UV to have a better surface quality. The 3D printer was a Desktop SLA resin printer (Formlabs, Form 2 Model) (Sabanci University Information Center, Sabanci University Information Center) and the resin is Gray Pro resin purchased from Formlabs company (Formlabs, Formlabs).
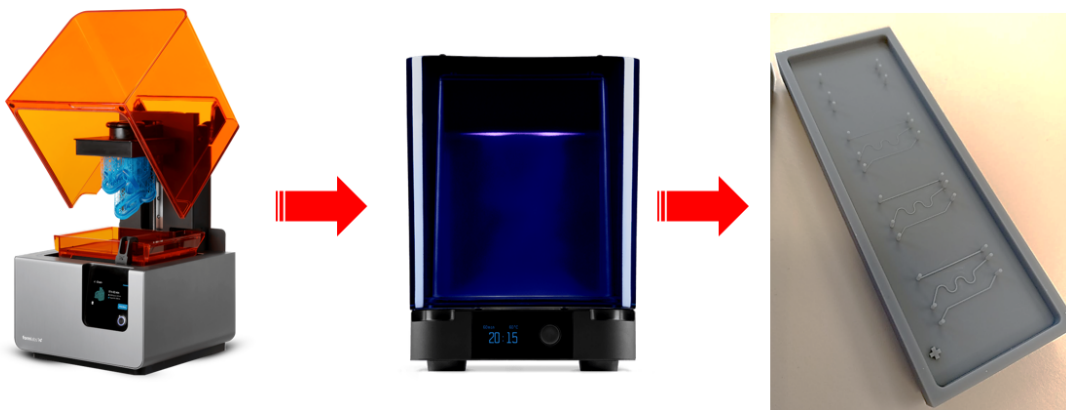
Figure 3.7 Process of preparing 3D printed molds

3.2.2 Chip material

Poly(dimethylsiloxane) (PDMS) is the most common material for the fabrication of microfluidic devices. It is a silicon-based elastomer having favorable properties like transparency, flexibility, gas permeability, biocompatibility, and low cost. Furthermore, from a microfabrication point of view, it is compatible with different techniques (Raj M & Chakraborty, 2020). Considering organ-on-chip applications, there are two drawbacks regarding using PDMS; the first absorbance of hydrophobic molecules which adversely affects drug screening studies (Winkler, Feil, Stronkman,

Matthiesen & Herland, 2020) and the slight fluorescent property of PDMS which can be eliminated by noise removal approaches (Piruska, Nikcevic, Lee, Ahn, Heineman, Limbach & Seliskar, 2005). Figure 3.8 summarizes both negative and positive features of PDMS.
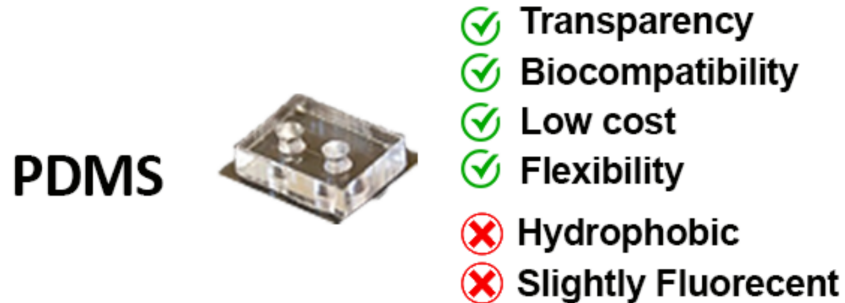
Figure 3.8 PDMS properties

Transparency, biocompatibility, molding capability, sterilization compatibility, low cost, and rapid prototyping are the main reasons why PDMS has been chosen for this research.

3.2.3 Chip fabrication and bonding

Having the mold ready, the same steps of soft lithography have been followed (Fig. 3.9). Inside the clean room, PDMS has been prepared with a 10:1 ratio (base and reagent) and degassed inside the chamber. The molds have been cleaned with Isopropyl Alcohol (IPA) and washed with distilled water. Finally, it dried with nitrogen. When the PDMS mixture has been fully degassed, it has been poured inside the mold and double-checked for bubbles, and moved inside the oven to be cured for at least 3 hours at 60°C.
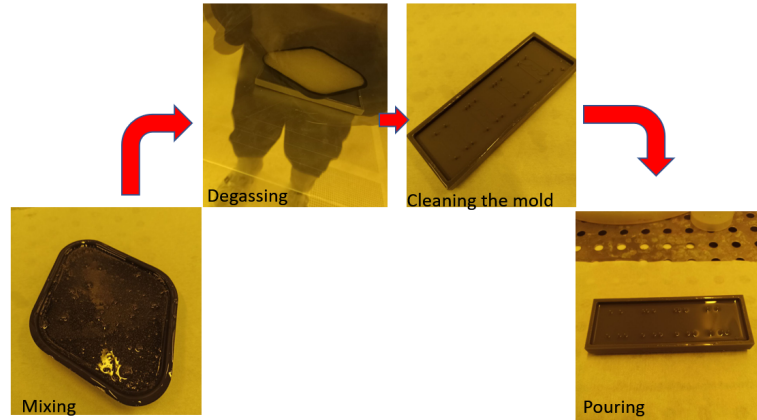
Figure 3.9 Degassing and Pouring PDMS

After curing it has been removed from the mold and stored properly not to have dust inside the channels.

Accordingly, for the bottom substrate, a thin flat layer of PDMS has been fabricated. The bonding of the two has been done by diffusing oxygen, applying plasma to the surfaces, and pushing them together. Figure 3.10 is showing the fabricated microfluidic devices.
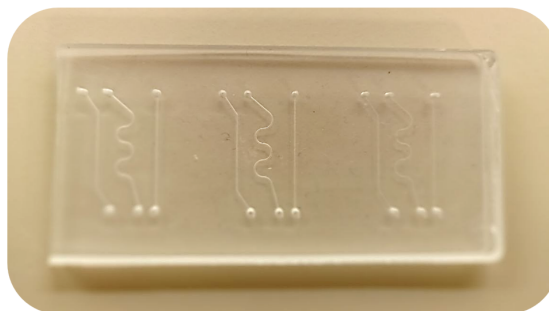
Figure 3.10 Fabricated PDMS chip

3.2.4 Surface characterization

In the next step, the fabricated chip was studied to learn the existing features and characteristics and improve them if necessary. Geometrical confinement and topographical features are categorized as passive mechanical stimuli and have previously been discussed. So, first, the roughness of PDMS substrate is studied which is a crucial parameter in organ chip models.

3.2.4.1 Surface roughness

Although 3D printing molds are an easy and fast approach, there are drawbacks that limit the method. The surface topology of the fabricated PDMS chips has high variability and roughness(Hwang, Seo, Roy, Han, Candler & Seo, 2016). Thus, in this study first, we measured the roughness of the surface of the channels with a profilometer.

The applied standard for measurement was ISO 25178 which is Geometrical Product Specifications (GPS). The measured terms are as follows:

Root mean square height is the standard deviation of heights. *Skewness* is representing how the roughness shape is biased (asperity); $S_{sk} = 0$ shows that height distribution (peaks & pits) is symmetrical considering the mean. Consequently, positive ($S_{sk} > 0$) and negative ($s_{sk} < 0$) indicate a height distribution below and above the mean (Figure 3.11 -A).

Kurtosis is a value that shows the sharpness of the roughness profile. In a normal distribution, the value of S_{ku} is 3. Sharp (spiked) distribution has higher S_{ku} ($S_{ku} > 3$) and softer distribution has lower S_{ku} ($S_{ku} < 3$) (figure 3.11-B).

Arithmetical mean height shows the difference of each point compared to the arithmetical mean of the surface and it is an essential parameter to assess the surface roughness.
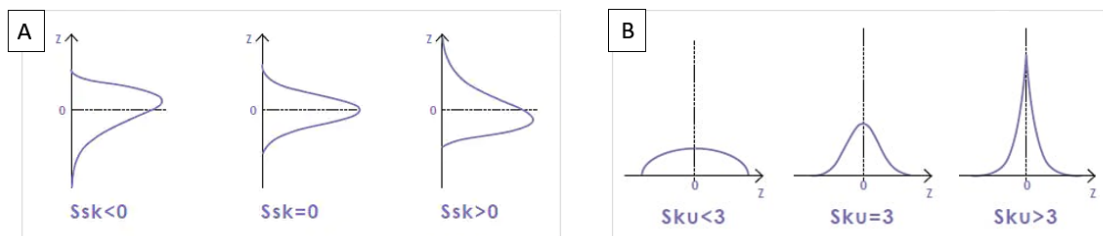
Figure 3.11 Skewness and Kurtosis distribution

3.3 Surface modification

Taking into account the hydrophobicity of PDMS (water contact angle > 100°), surface modification is necessary to make it a suitable environment for cells to attach and live (Trantidou, Elani, Parsons & Ces, 2017). In organ-on-chips, surface

treatment is for two purposes:

1- Correcting the hydrophobicity of PDMS

2- Providing extra-cellular matrix(ECM) for cells

There are a variety of methods proposed to reduce the hydrophobicity of PDMS. The results are different with respect to contact angle reduction (wettability) and durability, which are crucial parameters to consider. In this study, we attempted to reduce hydrophobicity by plasma treatment, UV treatment, silanization, and protein coating.

Plasma treatment is a fast approach by which ionized gas functionalizes the outer surface by dissociating and reacting with the substrate surface and is very common. This approach employs different gases, including oxygen, nitrogen, and hydrogen. The contact angle can be reduced down to 17°-18° just after exposure (considering different protocols) but will increase with time and returns to its original condition in 3 storage day(Ren, Bachman, Sims, Li & Allbritton, 2001).

Ultraviolet(UV) can be categorized as another method for oxidizing PDMS similar to plasma. Although UV treatment is considerably slower than plasma, it induces deeper modification to PDMS(Efimenko, Wallace & Genzer, 2002).

Silanization also can be applied on PDMS substrates since they contain surface hydroxyl groups. These hydroxyl groups will react with alkoxysilanes and make covalent Si-O-Si bonds. (3-aminopropyl)triethoxysilane (APTES) is a well-known alkoxysilane that is used as a solution after plasma surface activation (combination of plasma treatment & silanization)(Sui, Wang, Lee, Lu, Lee, Leyton, Wu & Tseng, 2006).
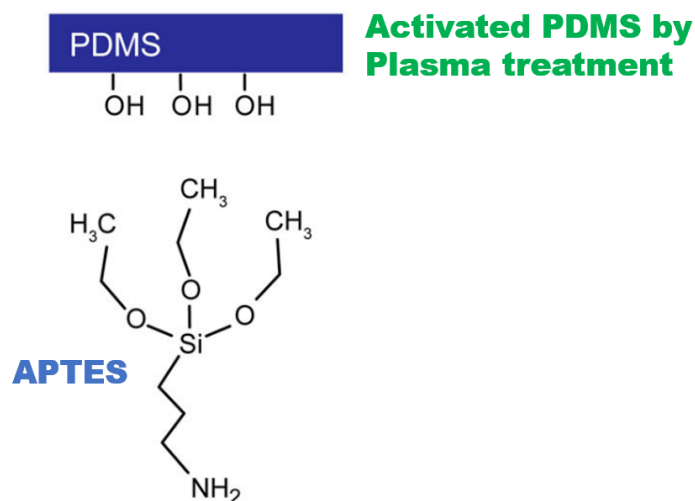
Figure 3.12 APTES-PDMS bonding

Proteins are also other surface modifiers. This approach has added advantages as it

increases biocompatibility. Hydrophobins, collagen, and fibronectin are among the classes of proteins used for surface modifications(Zhou, Ellis & Voelcker, 2010).

To investigate the best approach to achieve our goals to modify hydrophobicity and at the same time provide the ECM for the cells, six different samples have been checked for water contact angle. To do the experiment, 6 different PDMS parts have been treated in different ways and compared in contact angle. The selected coatings for this study are as follows (figure 3.13-B):

1- Untreated PDMS

2- Plasma treated PDMS

3- UV treated PDMS (10 min, 18W)

4- APTES coated

5- APTES+ Fibronectin + Collagen I

6- APTES + Fibronectin

For measurement, Theta lite optical tensiometer (figure 3.13- A) has been used and the amount of the droplet has been set to 5 μm. The contact angle has been obtained by the device image processing software and checked with ImageJ.
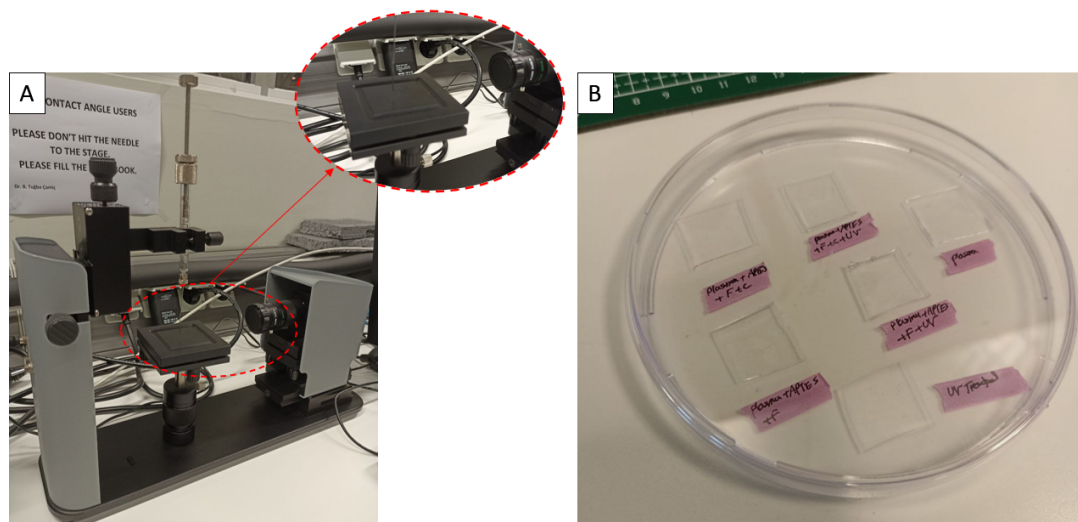
Figure 3.13 Samples and device for water contact angle measurement

3.4 Chip Sterilization

Different methods have been proposed in the literature to sterilize chips before cell seeding. Rinsing with ethanol and DI water is a common practice that needs to be done in adequate times (at least 3 times). UV exposure of chips is another

approach which there is a limitation for PDMS-made chips; the gas permeability of PDMS decreases with UV exposure which has a negative effect on uptaking CO_2 gas during the culturing in incubators. Figure 3.14 shows the UV treatment time vs. gas permeability of PDMS.
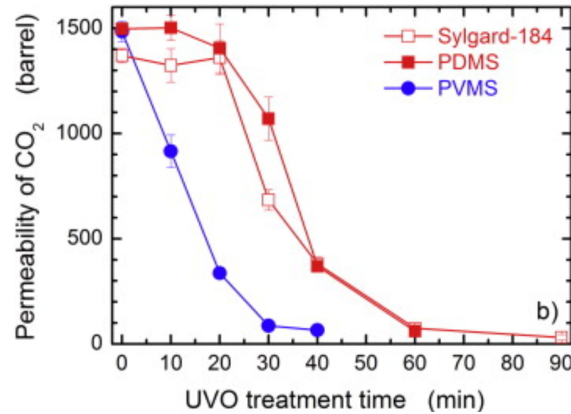
Figure 3.14 CO_2 permeability vs UV treatment in PDMS

In our study, since the chips are bonded just before use, they are treated with ozone plasma which makes them sterile (Oyama, Oyama & Taguchi, 2020).

3.5 Cell culturing and cell seeding

The employed cell line was Human umbilical vein endothelial cells (HUVEC) (gifted by Ege University) which are categorized as primary cells and isolated from the vein of the umbilical cord. They are usually used as the model for studying endothelial cells and their functions in several applications like inflammation and infection (Bordenave, Baquey, Bareille, Lefebvre, Lauroua, Guerin, Rouais, More, Vergnes & Anderson, 1993). Cells were cultured in 25 cm^2 flasks (T25)to have enough cells to do high-density cell seeding. The used media was RPMI 1640 (Gibco) plus ten percent Fetal Bovine Serum (FBS, PAN). Furthermore, non-essential amino acids (NEAA) and sodium pyruvate were added to the media, each was 1 %.

After the cells reached confluency, they were washed with DPBS (Dulbecco's phosphate-buffered saline) to remove dead cells and detached from the surface by Trypsin followed by a short incubation. Then, complete media were added and mixed well with the solution of the detached cells and trypsin. Cells were transferred to a 15 ml falcon tube and counted by a common hemocytometer. Having

known the cell numbers, they have been centrifuged. After centrifuging the cell pellet has been dissolved in a sufficient amount of media to make a density of 10,000 cell/μl.
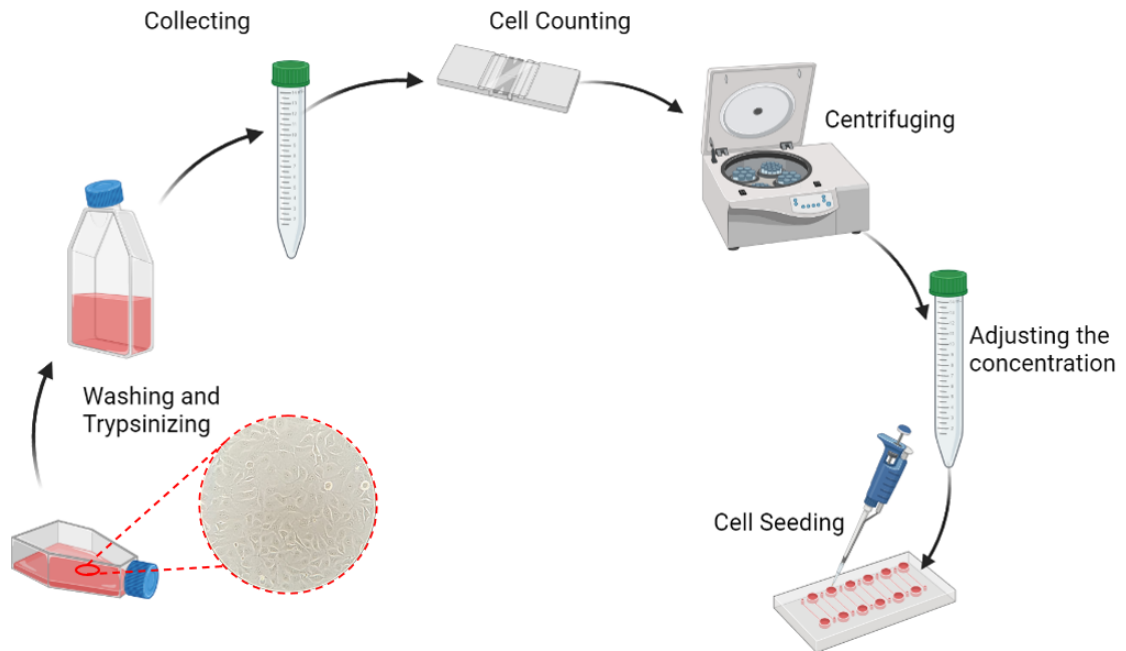
Figure 3.15 A schematic for cell seeding procedure

After observing that cells are attached, a peristaltic pump (Ismatech) has been connected to the chips as shown in figure 3.16 to expose the cells to shear stress with different conditions.
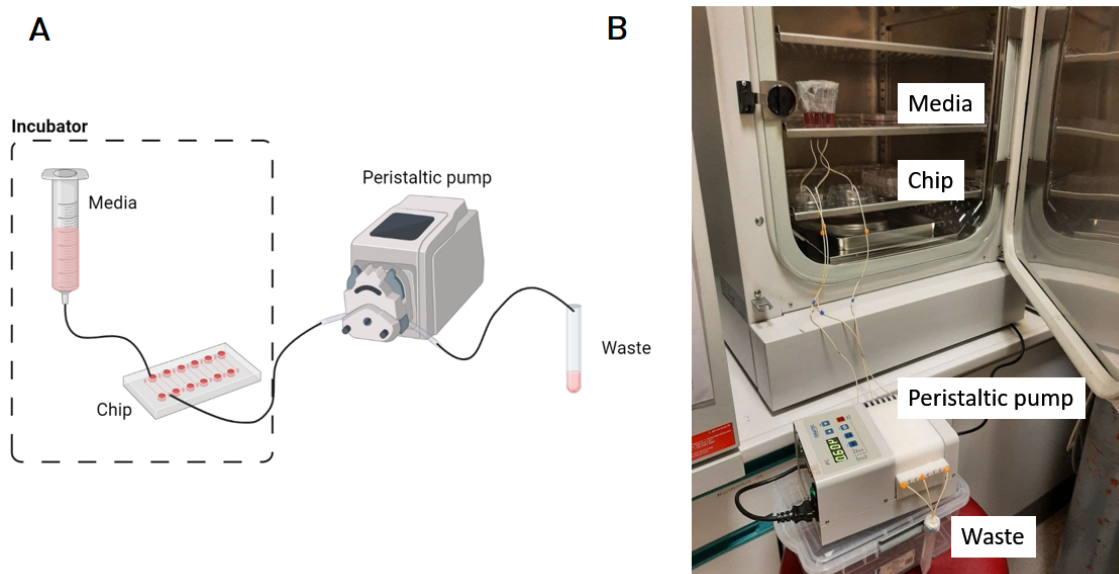
Figure 3.16 Experiment setup; A) schematic B) picture

3.6 Design of Experiment

To study the effect of viscosity, channel dimension, and curvature on the EC response, a set of experiments has been designed. Since our aim was to have a constant flow rate, in all experiments the flow rate was set on the $1\mu l/min$ driver by a peristaltic pump as a common flow rate and pattern in the pertinent literature. To investigate the *viscosity* effect, four different conditions have been considered. According to Section 2.3.1 blood viscosity is dependent on dimensions and hematocrit. Considering the average hematocrit and maximum arteries (300 μm) relative viscosity can be calculated as shown in figure 3.17
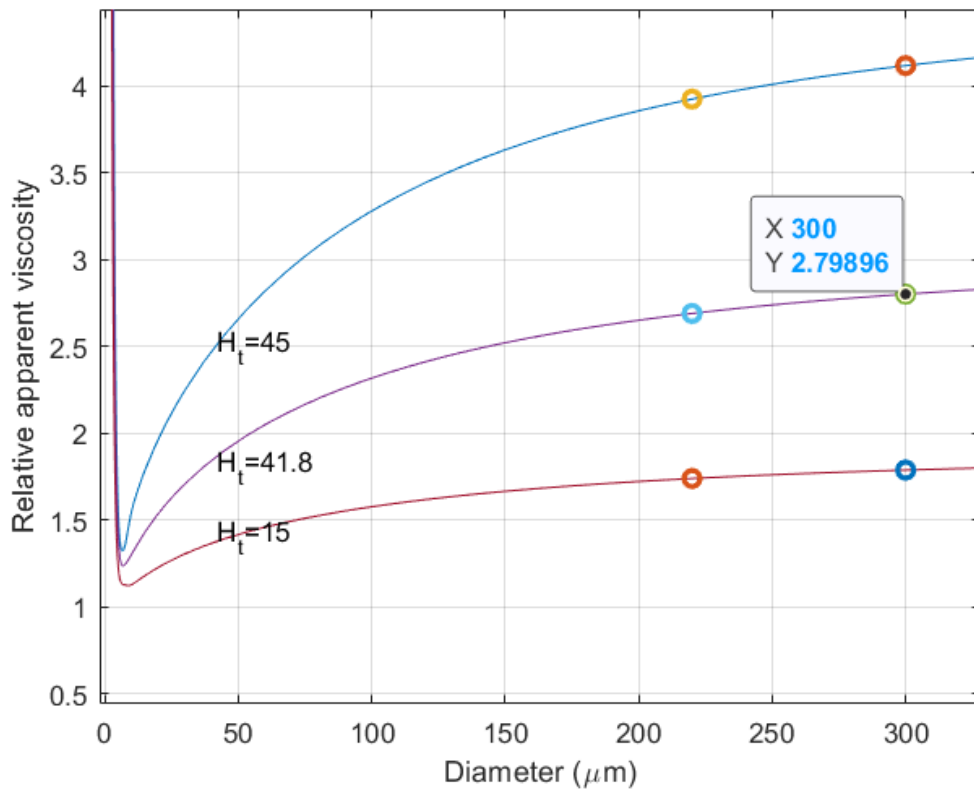
Figure 3.17 Relative viscosity of blood in $300\mu m$

Knowing the viscosity of plasma (suspending media) which is 1.2 *cp*, the viscosity of the blood will be 3.6 *cp* for this dimension. RPMI 1640 media with 10% FBS has a viscosity of 0.96 cp (Poon, 2022). To adjust other viscosities we used Dextran (M.W. 200,000 - 275,000) which has the viscosity per concentration as shown in figure 3.18. Considering an average molecular weight of 235,000, the viscosity per millimolar concentration is 7 cp (Gonzalez-Castillo, Rubio & Zenteno-Savin, 2003). The

experimental conditions have been considered as per table 3.2 for 0 mM, 0.2 mM, 0.4 mM and 0.6 mM of Dextran (M.W 200,000 -275,000, BDH) in cell culture media.
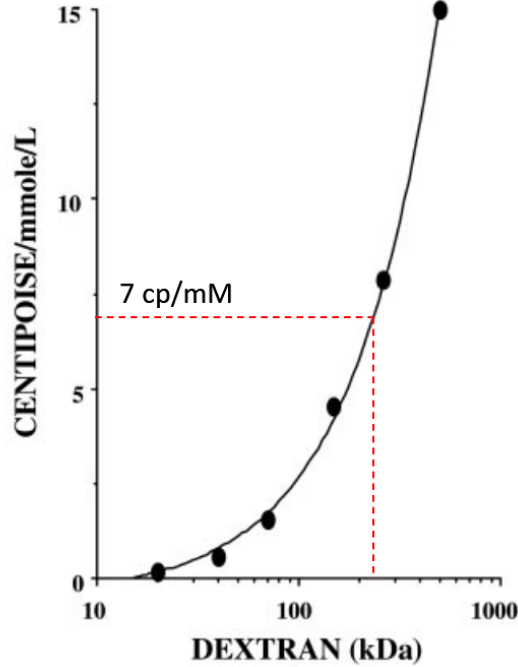
Figure 3.18 Dextran viscosity solutions in PBS

The experiment had 4 chips with dimensions of $300\mu m$ with a serpentine shape connected to the flow of media with adjusted viscosities. Also, the control group with the same channel features and media, but under static conditions (without flow). Accordingly, to study the cell response to dimension change and curvature,

Table 3.2 Experimental conditions to study viscosity effect

case	1	2	3	4
viscosity	0.96 cp	1.4 cp	2.8 cp	4.2 cp

a range of diameters has been selected considering the arteries' size. The studied sizes are 300 and $220\mu m$ which have both serpentine and straight channel geometries.

3.7 Numerical simulation

COMSOL Multiphysics (V 5.5) has been used to model and analyze flow inside the channels. Since Reynolds numbers are low and the viscous forces are dominant throughout the channel, the creeping model has been selected as a validated method.

3.8 Staining & visualization

To visualize and observe cell membrane Cell Tracking Red Dye Kit (ab269446) was used which enables to stain cells and track them for about 20 days. The dye is not toxic and will affect within 30min -3 hours of incubation (depending on the dilution). Here the dilution ratio of 1:50 has been used with 3 hours of incubation. Labeled cells can be visualized by fluorescent microscopy at a wavelength of 554-575 nm.

3.9 Image Processing

CellProfiler (version 3.1.9) is the main platform used for Image processing. The threshold of the image has been adjusted by the minimum cross entropy method and through a global strategy. Adjusted images have been set for object detection, the shape being the only parameter considered for distinguishing clumped objects and dividing lines between objects. To validate the method, a test shape with known dimensions (in pixels) has been designed. Figure 3.19 shows the good agreement between the exact and measured dimensions and also the capability of the method to divide the objects. The reported data are in $pixel/pixel^2$ which have been converted to μm knowing the scale of the microscopic images (0.36 μm/pixel).
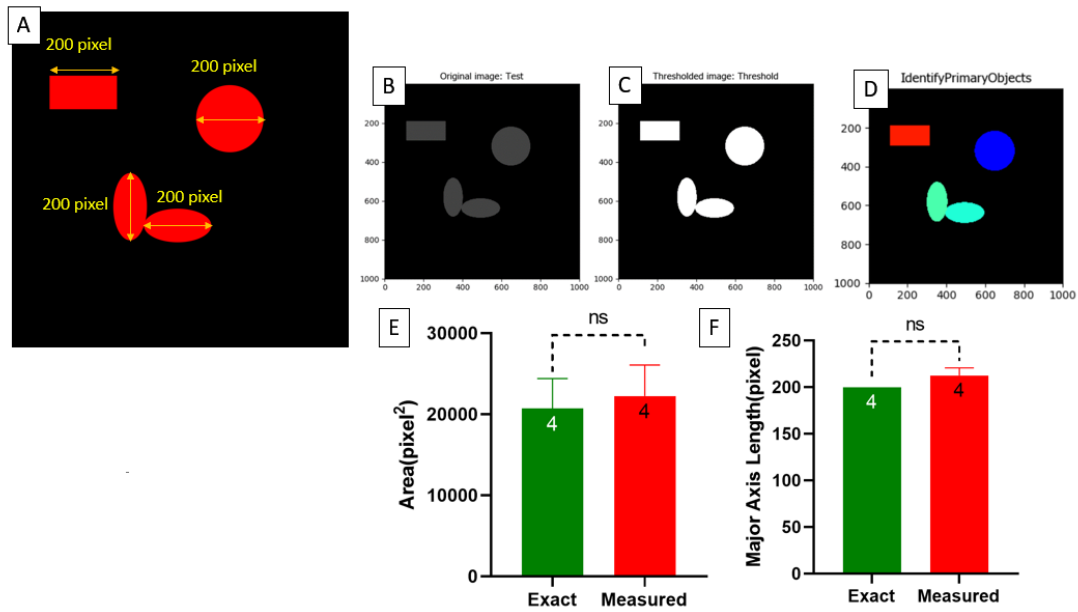
Figure 3.19 Comparison between the exact and measured object. A) is the input figure with designed objects, B) converting to grayscale, C) applying thresholding method, D) object detection, E)area comparison, F)Major axis length comparison.

3.10 Statistical analysis

The statistical analysis is two-way ANOVA. The two-way ANOVA compares the mean differences between groups that have been split into two independent variables (called factors). The primary purpose of a two-way ANOVA is to understand if there is an interaction between the two independent variables on the dependent variable. All data are represented by the mean and standard error of the mean (SEM) analyzed by Graphpad Prism (9.3.1).

3.11 Uncertainty analysis

There are uncertainties during the experiments arising from pump error, weighting device, and microfabrication, which have all been reported in table 3.3 extracted from the manufacturer's datasheet. The uncertainties of the derived parameters have

been calculated using Kline and McClintock method of error propagation (equation (3.3))Kline (1953)

$$U_p = \sqrt{\sum_{i=1}^{n}(\frac{\delta p}{\delta a_i}u_{a_i})^2} \tag{3.3}$$

Table 3.3 Uncertainties in variables

Uncertainty	Error
Flow rate, Q	1.0%
Weight measurement	$1 mg$
Volume measurement	0.1%
Channel dimension, a	±0.3%

4.   RESULTS

This chapter represents the results of the applied experiments and hypothesis. First, the chip characterization results are explained including the roughness measurement, surface modification by coating, flow analysis, and cell attachment. It has been followed by the results from studying EC cells inside and applying shear stress.

4.1 Surface roughness

Table 4.1 and figure 4.1 show the measured parameter and 3D topology of the substrate respectively. Measurement shows a distribution of rough features with an arithmetic mean of 1.3 μm. Skewness(S_{sk}) is positive indicating that height distribution is below the mean. Kurtosis(S_{ku}) is greater than 3 which shows that we have a sharp distribution of features (Figure 4.1- C and D).

Table 4.1 Surface roughness measurement

ISO 25178		
Height Parameters		
S_q (Root mean square height)	1619.66	nm
S_{sk} (Skewness)	1.15	
S_{ku} (Kurtosis)	4.03	
S_p (Maximum peak height)	5753.24	nm
S_v (Maximum pit height)	2690.28	nm
S_z (Maximum height)	8443.52	nm
S_a (Arithmetical mean height)	1256.27	nm
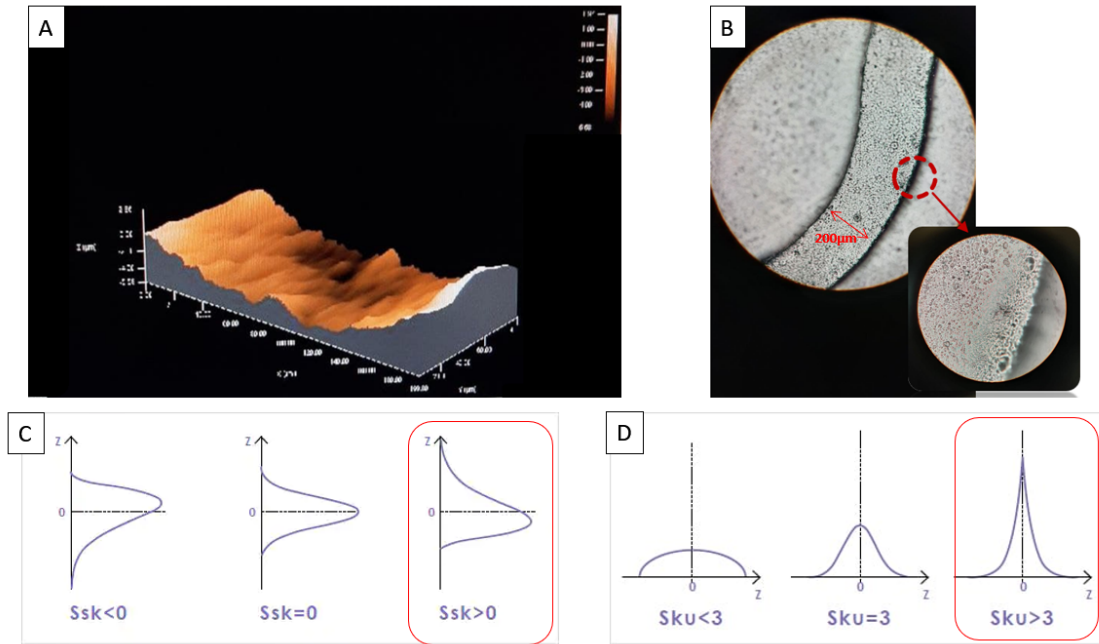
Figure 4.1 Substrate topology and graphical interpretation of the roughness terms S_{sk} and S_{ku}

The effects of the substrate's surface should be studied thoroughly since it is in direct contact with the flow, and as elaborated in Section 2.4.6 they could act as mechanical stimuli (passive). Therefore, the extracted data were used to model the substrate and see how the flow properties undergo changes. The results show that there is a high requirement to modify the surface since it induces fluctuations in the shear rate and the flow shear stress, as shown in the figure 4.2 obtained by numerical simulation.
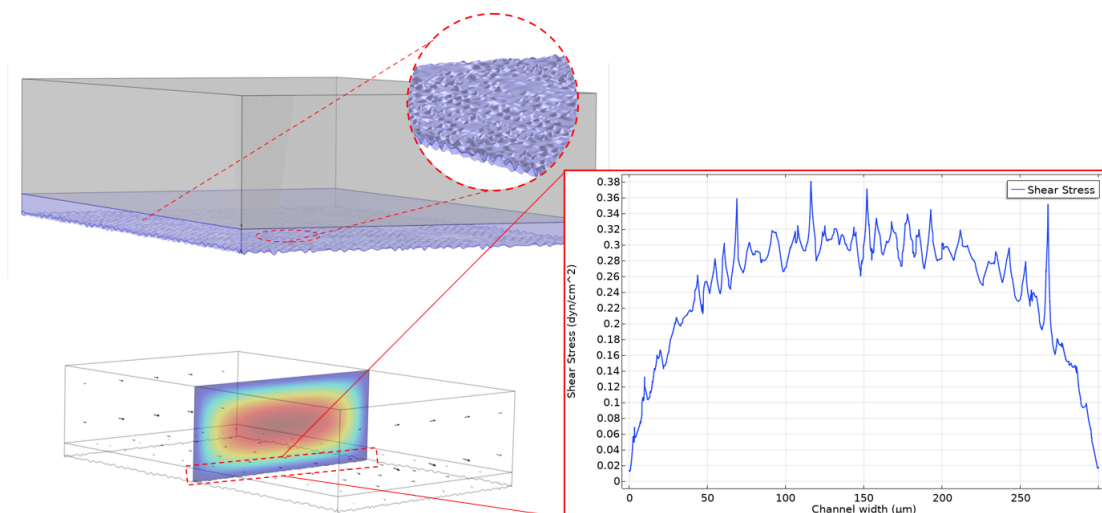
Figure 4.2 Shear stress fluctuation on rough surface

38

4.2 Hydrophilicity

Considering the shear fluctuation due to the roughness, the applied coating should satisfy three requirements; i) damping out the shear stress fluctuations ii) reducing PDMS intrinsic hydrophobicity, and iii) providing ECM for cells. The test outcome shows a promising function for the selected coatings. The results of untreated (4.3-A), APTES coated (4.3-B), Plasma treated (4.3-C) and UV treated (4.3-D) PDMS parts are consistent with the literature as shown in the following figure. There is a considerable reduction in the contact angle with the coatings, which is the result of the combination of silanization and proteins. Figure 4.3-E is an APTES coated surface with has been double coated with Fibronectin and Collagen I mixture. Figure 4.3-F is an APTES coated surface with only a Fibronecting coating.
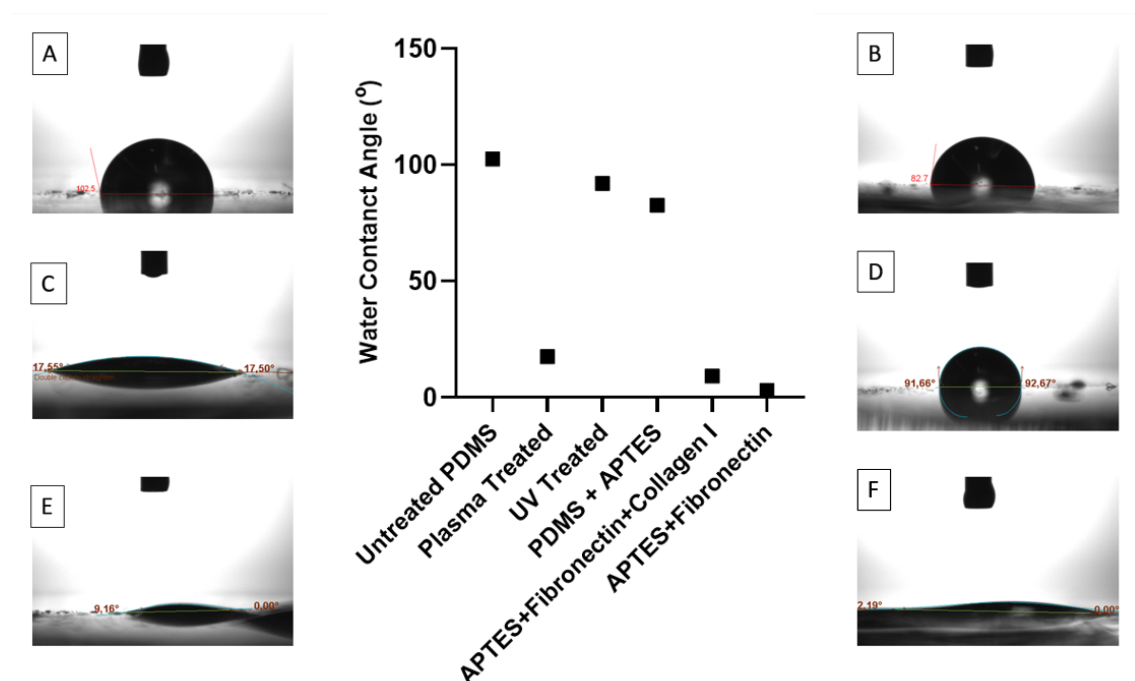
Figure 4.3 Measured contact angels; A) Pure PDMS B) APTES-coated C) Plasma treated D) UV treated E) APTES+Fibronectin+Collagen I F) APTES+Fibronectin

Accordingly, there are two choices to apply during the tests; APTES + mixture of Fibronectin & collagen-I and APTES + Fibronectin. Further studying of the coatings has been done inside the channels; the attachment of the cells and resistance to being washed by flow during the experiment are two other important criteria that will be mentioned in the next section (Section 4.3).

4.3 Cell attachment & stability

One of the most important preliminary goals of this research was finding a proper coating for PDMS substrate to supply ECM requirements for cells and at the same time stability in order to to be washed by the flow. To find the optimum coating, several experiments have been conducted. With only plasma, the number of attached cells is very few as it does not have a strong effect on the reduction and duration of hydrophilicity.

Although high concentration collagen type-I provides a suitable ECM for ECs for attachment and proliferation, it is prone to be washed by flow in long-term culture even if it is bound to APTES (Figure 4.4). Reducing collagen results in a low attachment rate.
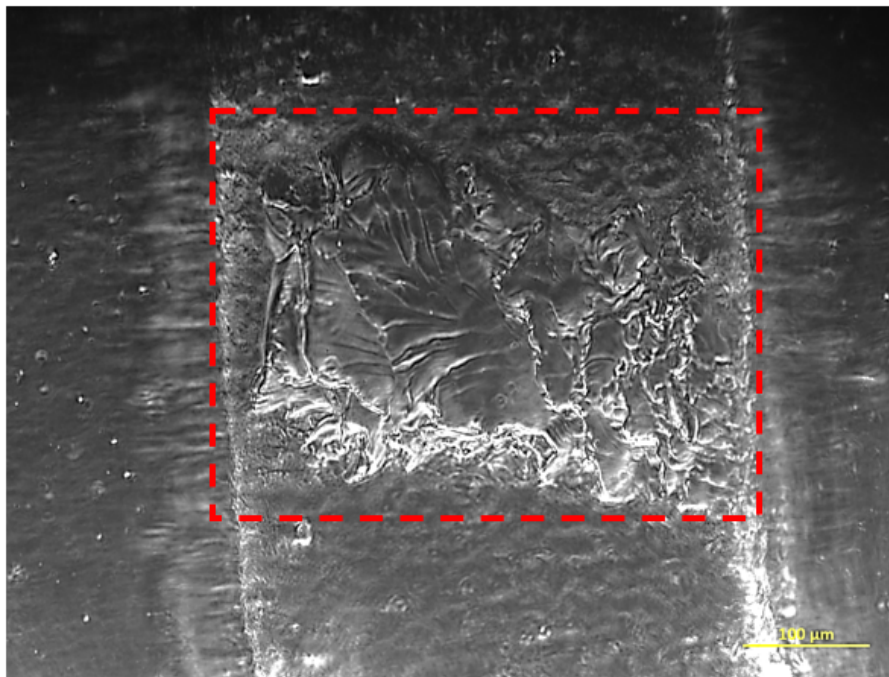
Figure 4.4 Clogging of the channel by Collagen; detached piece of collagen clogged the channel

On the other hand, Fibronectin is not holding a perfect binding with APTES as collagen does. However, the attachment is at an acceptable rate as shown in figure 4.5.
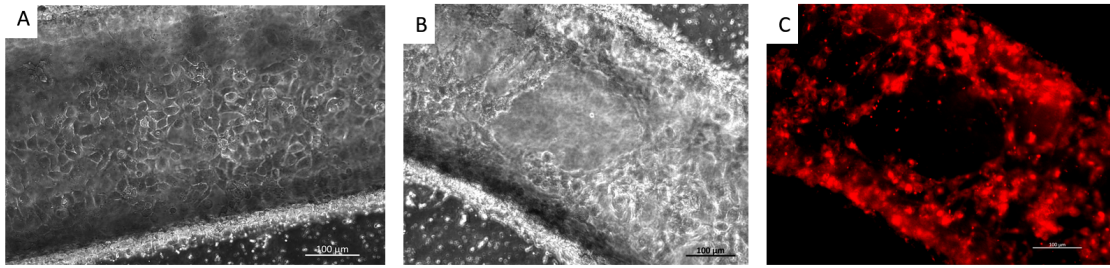
Figure 4.5 Static and flow condition with fibronectin coating. A) proper attachment of cells in static condition. B & C) a zone on the channel where the cells are detached from the substrate and accumulated.

Figure 4.5-A shows cell attachment after cell seeding, in which a confluent monolayer of cells can be observed. B is showing the channel after 24h flow which is stained in C demonstrating there is a loss of cells due to flow.

Accordingly, a mixture of Collagen-I and fibronectin have been used which not only reduces the contact angle but also binds perfectly with PDMS and is stable in the flow. This is also justifiable by the fact that in adventitia, type I collagen protects more fragile and smooth fibers and cells during high blood pressure (Zhang, 2020). Figure 4.6 shows cells condition in the channel after 48h flow
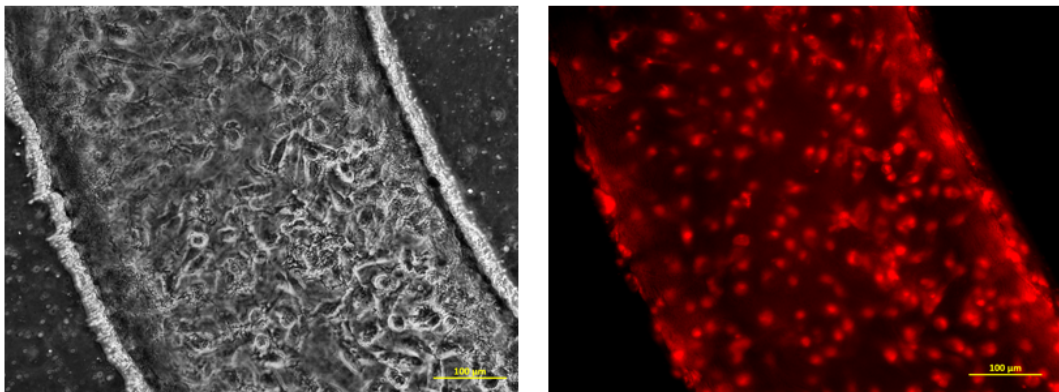
Figure 4.6 Stability of Collagen+ Fibronectin mixture

4.4 Viscosity effect

After preparing different concentrations of dextran in cell culture medium, eight chips have been prepared and coated for this experiment. All chips have the same dimension (300 μm) and also the same geometry (Serpentine). Four were used to apply shear and the other four were used to investigate static condition as shown in figure 4.7.
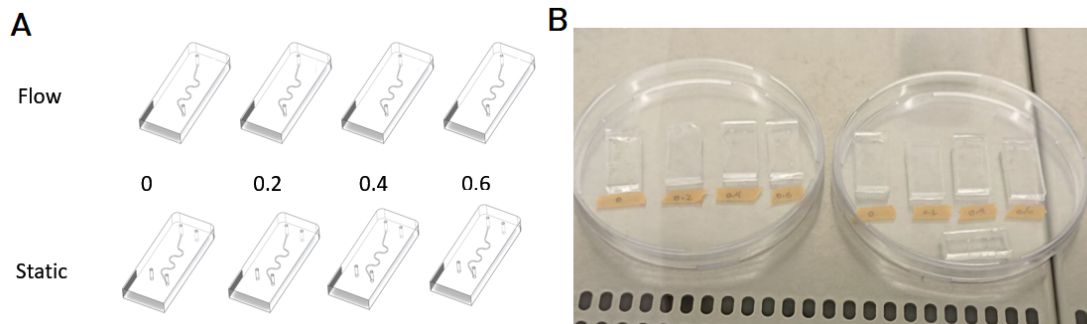
Figure 4.7 Viscosity experiment; four different concentrations of dextran 0, 0.2, 0.4, and 0.6 mM in both flow and static conditions A) schematic B) picture

To study how different amounts of viscosity expose different levels of shear stress with constant flow rate and dimension, the numerical model was applied and the shear stress (dyn/cm^2) was sketched along the length of the channel (Fig 4.8). The results show that viscosity not only changes the level of shear experienced by cells but also generates different shear gradients with respect to both time and position. Knowing the shear stress range (with a negligible uncertainty coming from the error propagation method), a 48-hour experiment was performed to apply the shears and then the cells were stained and visualized.
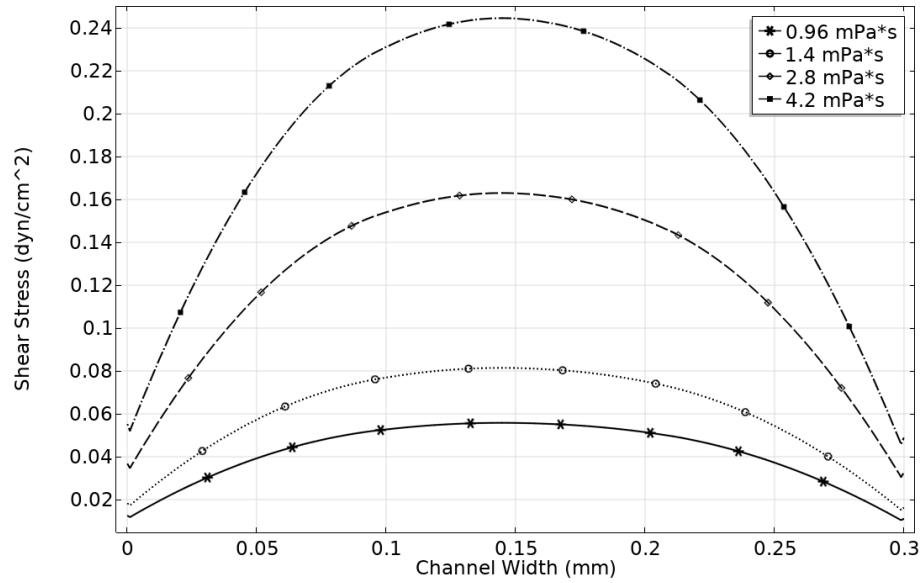
Figure 4.8 Numerical results (COMSOL) for shear stress with different viscosities with a flow rate of $1\mu l/\min$ in $300\mu m$ channel

In image processing, the parameters considered to observe morphology change were area and major axis change. The results show that there are changes both in the area and in the length of the major axis of the cells, although it is more significant for the area. Figure 4.9 shows the graphs for all four viscosity conditions and the difference between static and shear ones.
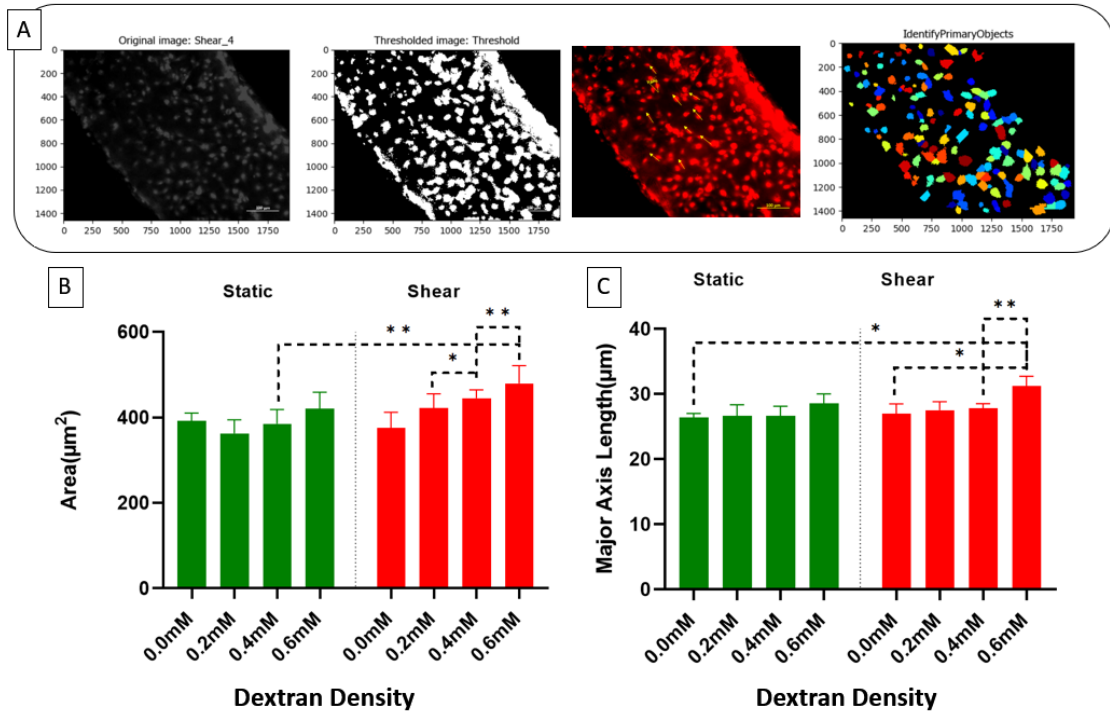
Figure 4.9 Area and major axis length change. A) Image processing example. B) Area change in different viscosities for both static and flow conditions. C) Changes in the major axis length of cells for different viscosities and static/flow conditions.

Figure 4.9-A demonstrates how the image processing is done for one case (0.4mM of Dextran) including thresholding of the image and object detection.

Significant changes are happening when the viscosity is changing and Accordingly, since mechanical forces are functions of time, magnitude, and frequency, for the second experiment 0.4mM concentration case has been selected and exposed to 72 hours of shear.
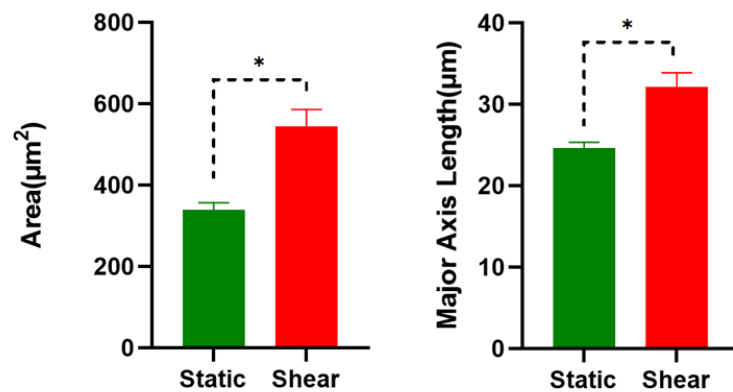
Figure 4.10 Morphological cell response to shear stress (0.16 dyn/cm^2) after 72 h (0.4 mM Dextran)

Figure 4.10 shows the area and major axis length change of the cells after 72 hours, which are significantly enhanced. Figure 4.11 is the comparison of parameters between 48 and 72 hours of shear exposure for a concentration of 0.4 mM dextran.
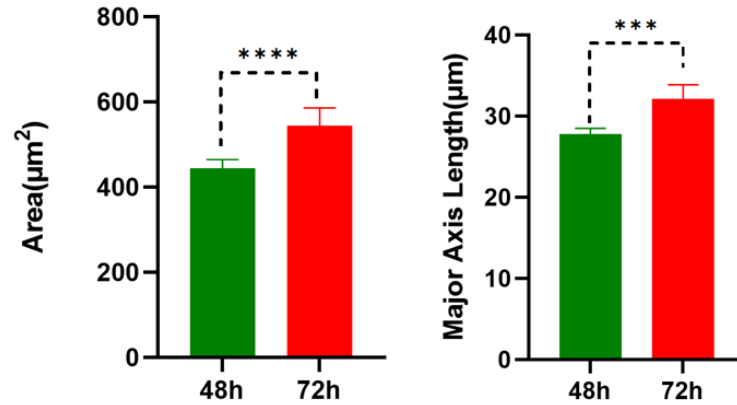
Figure 4.11 Comparison of 72h and 48h shear results(0.4mM of Dextran = 0.16 dyn/cm^2)

4.5 Dimension effect

Having the same flow rate and going down in the channel dimension is a challenging experience since the velocity of the media increases accordingly. On the other hand, the surface area for both coating and attaching the cells is smaller. Therefore, the first result can be reported as a high number of failures in experiments to expose them to shear.

The most reliable results are related to channels with the dimension of 220 μm. Figure 4.12 illustrates the change in the area and major axis length when the cells have been exposed to 48 h of shear stress with a normal cell culture medium (0 mM Dextran). There are no significant changes in the length of the major axis of the cells, but the area had a considerable increase.
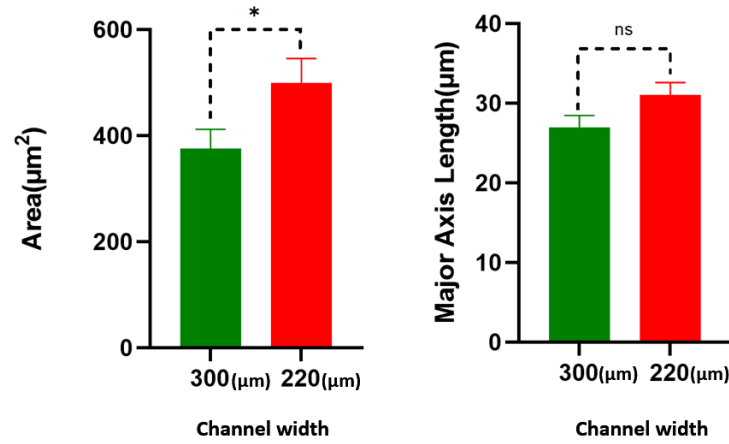
Figure 4.12 Comparison of morphological responses to dimension change

4.6 Curvature effect

Curvature study with the same parameters and comparing with the straight channel was another aspect of this study. The result shows that if the curvature is unfavorable for endothelial cells in vessels (high laminar shear stress), then its effects can be minimized by elongating along the vessel's length. Image processing data also proves cell morphology changes and responds to this physical property (Figure 4.13).

There is no significant change in 48h comparing the two geometries. But, in the numerical analysis of the channels, the straight one has a higher gradient of shear stress concerning the channel width. Also, there is a slightly higher shear rate because there is no resistance in the channel.
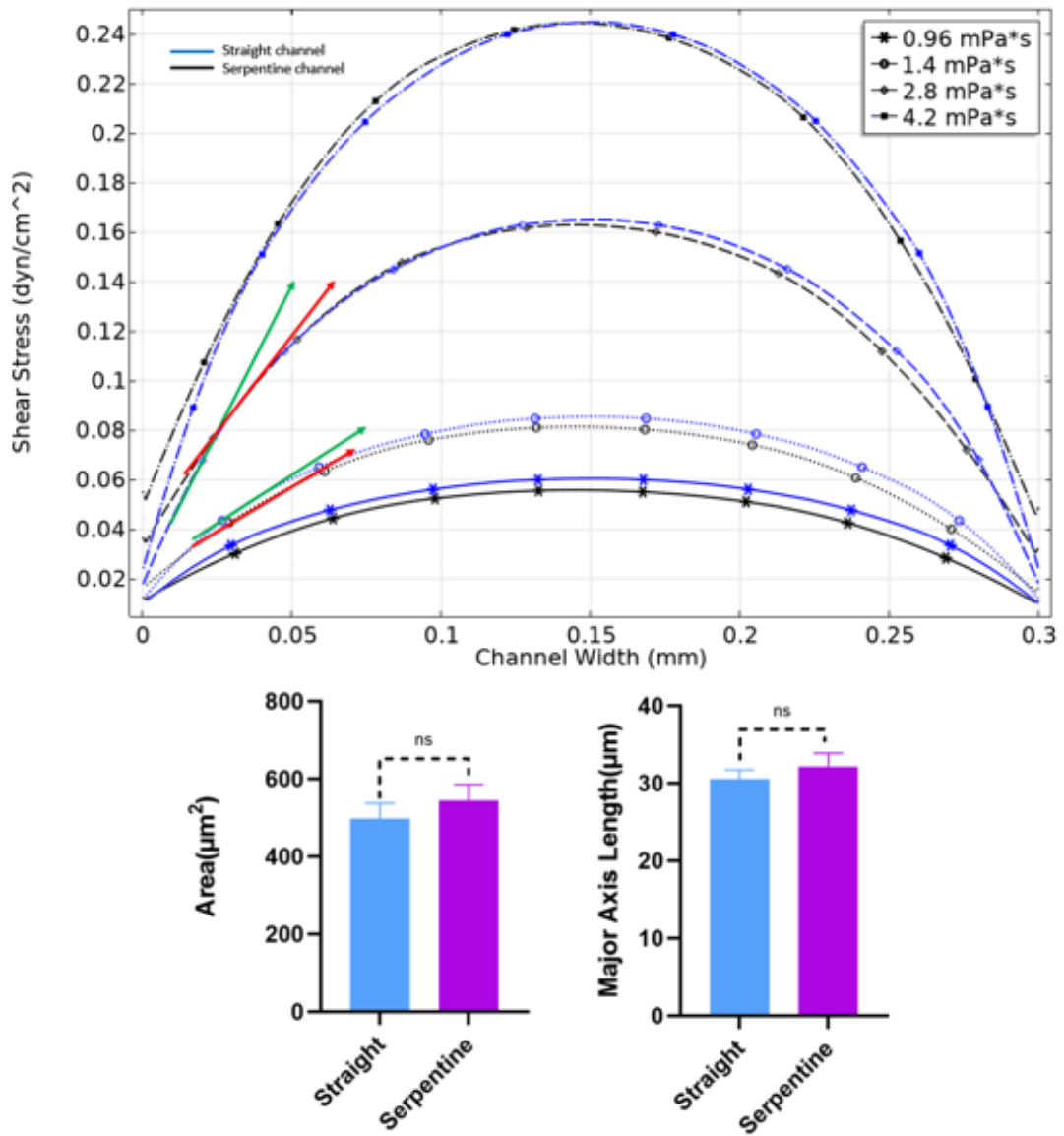
Figure 4.13 Comparison of straight and serpentine channels. The top graph compares the shear stress gradient of two geometries.

5. DISCUSSION

Evaluation of the results can begin with the chip function. Apart from the designing part, which is mostly reflected in the experiment outcome and will be discussed in the following, the important decision was the trade-off between the quality of the substrate and the speed of prototyping or cost. 3D printed molds provide acceptable microfluidic devices and the measured roughness is less than reported cases in the pertinent literature; Villegas et al. reported $2\mu m$ as the arithmetic mean (S_a) while here it is 1.26 μm(Villegas, Cetinic, Shakeri & Didar, 2018). Since there is a requirement to coat the substrates to modify the surface and also provide ECM for cells, there is no concern for the roughness features. Besides, the 3D printed mold has pillars in the place of the inlet and outlet, and the design size is matched with tubing and connection sizes which is beneficial in the experimental setups. Moreover, wall-edged molds make the chip have a specific and controllable height. The provided coating meets both the needs considered in the research; the seeded cells are attached at an acceptable rate and in a short period of time and are also stable during exposure to flow. Contact angel measurements also support the function of coatings to reduce hydrophobicity as a long-term solution.

Shear characterization results show that cells are more interacting by morphological responses to higher viscosities at a constant flow rate. The observed results show that cells grow in their size but not significantly in one direction (major axis).

Decreasing dimensions show not a significant response by cells although it is correlated with a cubic term in the formula and it can be also stated that their function is adversely affected.

The curvature also during the tested time exposure did not have a significant role but there are changes that make it noticeable since it is a real condition of the vasculature.

No signs of polarization or alignment have been observed in long-term shear stress (figure 5.1). This is also justified by the literature in which a low passage number and a preferred level of shear stress (set point) are mentioned as the conditions for polarization response (Baeyens, Nicoli, Coon, Ross, Van den Dries, Han, Lauridsen, Mejean, Eichmann, Thomas & others, 2015). This can be the subject of

further study in the future with fresh EC that differentiates from stem cells such as mesenchymal.
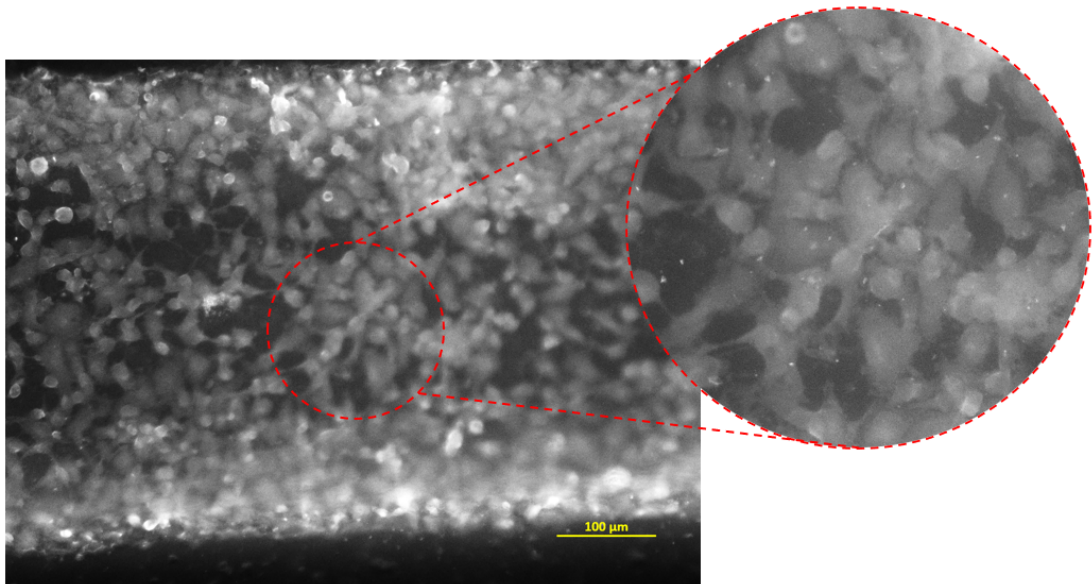
Figure 5.1 +72h shear exposure with 0.4 mM media. No sign of considerable alignment

The shear gradient effect is another important observed parameter in this regard. According to the literature, EC function is considerably reduced by laminar shear stress and will stop in the G0 and G1 phases of the cell cycle (Shigeo, 2000). But, the gradient of shear stresses helps their function and proliferation therefore oscillatory flow pattern has been proposed.

Here shear stress has been increased in two distinct ways; viscosity and also velocity (low dimensions). Observations are suggesting two different shear gradients and only one of them is favorable to ECs. Viscosity-dominated (low-inertia) shear stress imposes a high space-gradient shear on the ECs, which is favorable. Figure 5.2 shows two different pattern of shear. On the bigger channel, the shear change with time in each pulse of the flow (the peak) is comparably lower, but the shear gradient is changing considerably along the channel. On the edge sides, this gradient is higher and is decreasing through the middle zone.
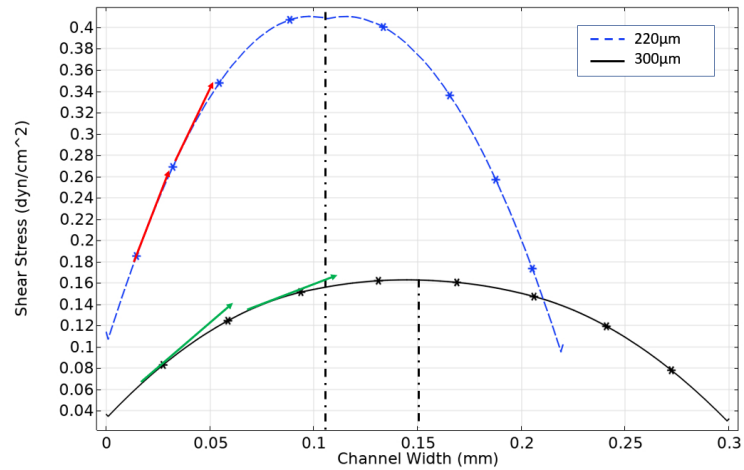
Figure 5.2 Shear stress distribution along the width of the channel for $220\mu m$ and $300\mu m$ with (0.4mM Dextran)

As shown in figure 5.3 the side zone of channels is more confluent of comparing to the middle zone in viscosity-dominated shear exposure. This happens while in lower dimensions (higher velocities), cells cannot adapt to the shear in the side zones. This also supports the number of high failures when reducing the dimensions. The result is also comparable with the body's natural response, as elaborated in section 2.3, and how blood reduces viscosity when the dimension is going down.

It is also worth mentioning that comparing the EC line to another cell line, U-87, which is a cancer cell, there was not such a sensitive behavior to shear stress and the cell function response was positive to all shear included experiments.
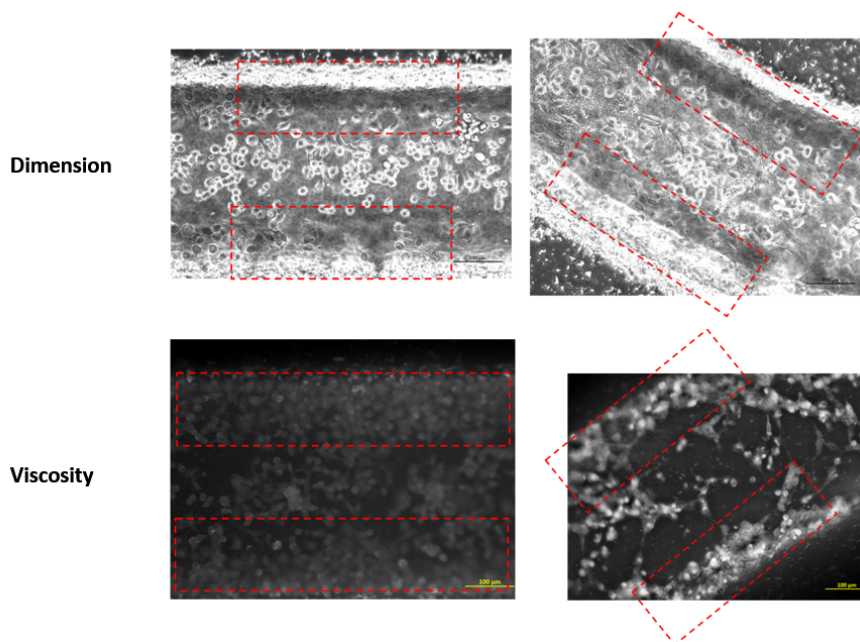
Figure 5.3 Effect of different shear gradients on ECs

6. CONCLUSION & FUTURE WORK

To model a vasculature on a chip, a microfluidic device has been fabricated by soft lithography and the mold has been 3D printed in accordance with the decision for the trade-off between surface roughness and prototyping time and cost. Further studies on the surface showed an acceptable roughness amount compared to that in the pertinent literature. In order to smooth the surface and damp out shear stress oscillations, a coating with APTES + collagen type I + fibronectin was applied not only to decrease the roughness but also to provide an ECM for attachment and proliferation of cells. The coating also helps cell attachment by reducing the hydrophobicity

In the experiments with cells, it has been observed that ECs are very sensitive to shear stress and start with a slight change in morphology to total cell function. Therefore, following our research question about inducing near physiological shear stress in organ-on-chip models with low flow rates, the feasibility of the experiments is another parameter to ponder. The reduction of channel dimensions adversely affects substrate coating and cell seeding. This is while in case of successful initiation of the experiment since the velocity of flow is higher, there is a high gradient of shear stress (concerning time) on ECs. Viscosity modification has promising results both in morphological responses and functions of EC. By viscosity-dominated shear exposure, ECs undergo a high space gradient of shear stress with pulsatile flow. The difference between these two shear gradients is also a new observation in the field, which will be further studied by other molecular assays such as western blot and q-PCR.

The fabrication process of this research can be replicated by other microfluidic applications knowing the quality of the produced surface which results in attenuation of time and cost. The obtained results in the coating part can be useful for those researchers working on PDMS microfluidic devices; employing silanization and protein coatings to reduce the water contact angle which is also privileged in the case of biocompatible applications. Also, the coating is promising for long-term cell culture inside PDMS channels. The final conclusion about the viscosity modification and shear gradients is a noticeable point when ECs are being used in organ-on-chips. In-

creasing shear stress by modification of viscosity can improve the micro-physiological environment (close to *in vivo*) and also the cell function.

Several future studies can be proposed according to the obtained results. To further study the shear and shear gradient effect on the cell responses, biological assays will be designed including protein analysis (western blot) and gene expression analysis (quantitative real-time PCR). The outcome might result in finding clues about some diseases and organ functions. This might also solve the limitations of image processing. Furthermore, to have a deeper understanding of real *in vivo* conditions, human blood can be perfused inside the microfluidic channels.

BIBLIOGRAPHY

Ahmadi, V. E., Butun, I., Altay, R., Bazaz, S. R., Alijani, H., Celik, S., Warkiani, M. E., & Koşar, A. (2021). The effects of baffle configuration and number on inertial mixing in a curved serpentine micromixer: Experimental and numerical study. *Chemical Engineering Research and Design*, *168*, 490–498.

Alevriadou, B. R., Eskin, S. G., McIntire, L. V., & Schilling, W. P. (1993). Effect of shear stress on86rb+ efflux from calf pulmonary artery endothelial cells. *Annals of biomedical engineering*, *21*(1), 1–7.

Aljohani, W., Ullah, M. W., Zhang, X., & Yang, G. (2018). Bioprinting and its applications in tissue engineering and regenerative medicine. *International journal of biological macromolecules*, *107*, 261–275.

Ando, J., Komatsuda, T., & Kamiya, A. (1988). Cytoplasmic calcium response to fluid shear stress in cultured vascular endothelial cells. *In vitro cellular & developmental biology*, *24*(9), 871–877.

Ashammakhi, N., Nasiri, R., De Barros, N. R., Tebon, P., Thakor, J., Goudie, M., Shamloo, A., Martin, M. G., & Khademhosseini, A. (2020). Gut-on-a-chip: Current progress and future opportunities. *Biomaterials*, *255*, 120196.

Baeyens, N., Bandyopadhyay, C., Coon, B. G., Yun, S., & Schwartz, M. A. (2016). Endothelial fluid shear stress sensing in vascular health and disease. *The Journal of Clinical Investigation*, *126*(3), 821–828.

Baeyens, N., Nicoli, S., Coon, B. G., Ross, T. D., Van den Dries, K., Han, J., Lauridsen, H. M., Mejean, C. O., Eichmann, A., Thomas, J.-L., et al. (2015). Vascular remodeling is governed by a vegfr3-dependent fluid shear stress set point. *elife*, *4*.

Bauer, R. D., Busse, R., & Schabert, A. (1982). Mechanical properties of arteries. *Biorheology*, *19*(3), 409–424.

Benam, K. H., Villenave, R., Lucchesi, C., Varone, A., Hubeau, C., Lee, H.-H., Alves, S. E., Salmon, M., Ferrante, T. C., Weaver, J. C., et al. (2016). Small airway-on-a-chip enables analysis of human lung inflammation and drug responses in vitro. *Nature methods*, *13*(2), 151–157.

Bordenave, L., Baquey, C., Bareille, R., Lefebvre, F., Lauroua, C., Guerin, V., Rouais, F., More, N., Vergnes, C., & Anderson, J. (1993). Endothelial cell compatibility testing of three different pellethanes. *Journal of biomedical materials research*, *27*(11), 1367–1381.

Bosman, F. T. & Stamenkovic, I. (2003). Functional structure and composition of the extracellular matrix. *The Journal of Pathology: A Journal of the Pathological Society of Great Britain and Ireland*, *200*(4), 423–428.

Chan, C. Y., Huang, P.-H., Guo, F., Ding, X., Kapur, V., Mai, J. D., Yuen, P. K., & Huang, T. J. (2013). Accelerating drug discovery via organs-on-chips. *Lab on a Chip*, *13*(24), 4697–4710.

Chien, S. (2007). Mechanotransduction and endothelial cell homeostasis: the wisdom of the cell. *American Journal of Physiology-Heart and Circulatory Physiology*, *292*(3), H1209–H1224. PMID: 17098825.

Chien, S. (2008). Effects of disturbed flow on endothelial cells. *Annals of biomedical engineering*, *36*(4), 554–562.

Chien, S., Li, S., & Shyy, J. Y. (1998). Effects of mechanical forces on signal transduction and gene expression in endothelial cells. *Hypertension*, *31*(1), 162–169.

Chien, S. C. (1975). Chapter 26 – biophysical behavior of red cells in suspensions.

DeOre, B. J., Partyka, P. P., Fan, F., & Galie, P. A. (2022). Cd44 mediates shear stress mechanotransduction in an in vitro blood-brain barrier model through small gtpases rhoa and rac1. *The FASEB Journal*, *36*(5), e22278.

Dersoir, B., de Saint Vincent, M. R., Abkarian, M., & Tabuteau, H. (2015). Clogging of a single pore by colloidal particles. *Microfluidics and Nanofluidics*, *19*(4), 953–961.

Dincau, B., Dressaire, E., & Sauret, A. (2020). Pulsatile flow in microfluidic systems. *Small*, *16*(9), 1904032.

Dressaire, E. & Sauret, A. (2017). Clogging of microfluidic systems. *Soft matter*, *13*(1), 37–48.

Efimenko, K., Wallace, W. E., & Genzer, J. (2002). Surface modification of sylgard-184 poly (dimethyl siloxane) networks by ultraviolet and ultraviolet/ozone treatment. *Journal of colloid and interface science*, *254*(2), 306–315.

Fiorini, G. S. & Chiu, D. T. (2005). Disposable microfluidic devices: fabrication, function, and application. *BioTechniques*, *38*(3), 429–446.

Formlabs. Grey Pro Resin. online: `https://formlabs.com/eu/materials/standard/#grey-pro-resin`. Accessed: 2022-06-15.

Gonzalez-Castillo, C., Rubio, R., & Zenteno-Savin, T. (2003). Coronary flow-induced inotropism is modulated by binding of dextrans to the endothelial luminal surface. *American Journal of Physiology-Heart and Circulatory Physiology*, *284*(4), H1348–H1357.

Haase, K. & Kamm, R. D. (2017). Advances in on-chip vascularization. *Regenerative medicine*, *12*(3), 285–302.

Harris, J. R. & Korolchuk, V. I. (2019). *Biochemistry and Cell Biology of Ageing: Part II Clinical Science*. Springer.

Hill, M. A. & Meininger, G. A. (2012). Chapter 93 - myogenic tone and mechanotransduction. In J. A. Hill & E. N. Olson (Eds.), *Muscle* (pp. 1243–1257). Boston/Waltham: Academic Press.

Howell, Jr., P. B., Mott, D. R., Fertig, S., Kaplan, C. R., Golden, J. P., Oran, E. S., & Ligler, F. S. (2005). A microfluidic mixer with grooves placed on the top and bottom of the channel. *Lab Chip*, *5*, 524–530.

Humphrey, J. (2008). Vascular adaptation and mechanical homeostasis at tissue, cellular, and sub-cellular levels. *Cell biochemistry and biophysics*, *50*(2), 53–78.

Humphrey, J. D. & Delange, S. L. (2004). An introduction to biomechanics. *Solids and Fluids, Analysis and Design. Springer, Heidelberg*.

Humphrey, J. D. & Schwartz, M. A. (2021). Vascular mechanobiology: homeostasis, adaptation, and disease. *Annual Review of Biomedical Engineering*, *23*, 1–27.

Hwang, Y., Seo, D., Roy, M., Han, E., Candler, R. N., & Seo, S. (2016). Capillary flow in pdms cylindrical microfluidic channel using 3-d printed mold. *Journal of Microelectromechanical Systems*, *25*(2), 238–240.

Ingber, D. E. (2020). Is it time for reviewer 3 to request human organ chip experiments instead of animal validation studies? *Advanced Science*, *7*(22), 2002030.

Javris, S. (2018). Vascular system 1: anatomy and physiology. *Nursing Times*,

114(4), 40–44.

Karthika, C., Ahalya, S., Radhakrishnan, N., Kartha, C., & Sumi, S. (2021). Hemodynamics mediated epigenetic regulators in the pathogenesis of vascular diseases. *Molecular and Cellular Biochemistry*, *476*(1), 125–143.

Kim, J., Antaki, J. F., & Massoudi, M. (2016). Computational study of blood flow in microchannels. *Journal of Computational and Applied Mathematics*, *292*, 174–187.

Kim, J., Lee, C., Kim, I., Ro, J., Kim, J., Min, Y., Park, J., Sunkara, V., Park, Y.-S., Michael, I., et al. (2020). Three-dimensional human liver-chip emulating premetastatic niche formation by breast cancer-derived extracellular vesicles. *ACS nano*, *14*(11), 14971–14988.

Kim, S., Lee, H., Chung, M., & Jeon, N. L. (2013). Engineering of functional, perfusable 3d microvascular networks on a chip. *Lab on a Chip*, *13*(8), 1489–1500.

Kline, S. J. (1953). Describing uncertainty in single sample experiments. *Mech. Engineering*, *75*, 3–8.

Kuchan, M. & Frangos, J. (1993). Shear stress regulates endothelin-1 release via protein kinase c and cgmp in cultured endothelial cells. *American Journal of Physiology-Heart and Circulatory Physiology*, *264*(1), H150–H156.

Lee, J.-H., Park, H.-K., & Kim, K. S. (2016). Intrinsic and extrinsic mechanical properties related to the differentiation of mesenchymal stem cells. *Biochemical and Biophysical Research Communications*, *473*(3), 752–757. Special Issue: Stem Cells.

Lee, S., Chung, M., Lee, S.-R., & Jeon, N. L. (2020). 3d brain angiogenesis model to reconstitute functional human blood-brain barrier in vitro. *Biotechnology and bioengineering*, *117*(3), 748–762.

Lesman, A., Rosenfeld, D., Landau, S., & Levenberg, S. (2016). Mechanical regulation of vascular network formation in engineered matrices. *Advanced Drug Delivery Reviews*, *96*, 176–182.

Levesque, M., Nerem, R., & Sprague, E. (1990). Vascular endottielial cell proliferation in culture and the influence of flow. *Biomaterials*, *11*(9), 702–707.

Li, Y.-S. J., Haga, J. H., & Chien, S. (2005). Molecular basis of the effects of shear stress on vascular endothelial cells. *Journal of biomechanics*, *38*(10), 1949–1971.

Lim, C. T., Bershadsky, A., & Sheetz, M. P. (2010). Mechanobiology. *Journal of the Royal Society, Interface*, *7 Suppl 3*(Suppl 3), S291–S293.

Lu, R. X. Z., Lai, B. F. L., Rafatian, N., Gustafson, D., Campbell, S. B., Banerjee, A., Kozak, R., Mossman, K., Mubareka, S., Howe, K. L., et al. (2022). Vasculature-on-a-chip platform with innate immunity enables identification of angiopoietin-1 derived peptide as a therapeutic for sars-cov-2 induced inflammation. *Lab on a Chip*, *22*(6), 1171–1186.

Ma, C., Peng, Y., Li, H., & Chen, W. (2021). Organ-on-a-chip: a new paradigm for drug development. *Trends in pharmacological sciences*, *42*(2), 119–133.

Malek, A. & Izumo, S. (1996). Mechanism of endothelial cell shape change and cytoskeletal remodeling in response to fluid shear stress. *Journal of Cell Science*, *109*(4), 713–726.

Mitsumata, M. (1991). Shear stress inhibits endothelial cell proliferation by growth arrest in the g_0/g_1 phase of the cell cycle. *FASEB J.*, *5*, A527.

Morris, A. J. & Malbon, C. C. (1999). Physiological regulation of g protein-linked signaling. *Physiological reviews*, *79*(4), 1373–1430.

Osawa, M., Masuda, M., Kusano, K.-i., & Fujiwara, K. (2002). Evidence for a role of platelet endothelial cell adhesion molecule-1 in endothelial cell mechanosignal transduction: is it a mechanoresponsive molecule? *The Journal of cell biology*, *158*(4), 773–785.

Oyama, T. G., Oyama, K., & Taguchi, M. (2020). A simple method for production of hydrophilic, rigid, and sterilized multi-layer 3d integrated polydimethylsiloxane microfluidic chips. *Lab Chip*, *20*, 2354–2363.

Park, T. E., Mustafaoglu, N., Herland, A., Hasselkus, R., Mannix, R., FitzGerald, E. A., Prantil-Baun, R., Watters, A., Henry, O., Benz, M., Sanchez, H., McCrea, H. J., Goumnerova, L. C., Song, H. W., Palecek, S. P., Shusta, E., & Ingber, D. E. (2019). Hypoxia-enhanced Blood-Brain Barrier Chip recapitulates human barrier function and shuttling of drugs and antibodies. *Nature Communications*, *10*(1), 1–12.

Partyka, P. P., Godsey, G. A., Galie, J. R., Kosciuk, M. C., Acharya, N. K., Nagele, R. G., & Galie, P. A. (2017). Mechanical stress regulates transport in a compliant 3d model of the blood-brain barrier. *Biomaterials*, *115*, 30–39.

Piruska, A., Nikcevic, I., Lee, S. H., Ahn, C., Heineman, W. R., Limbach, P. A., & Seliskar, C. J. (2005). The autofluorescence of plastic materials and chips measured under laser irradiation. *Lab on a Chip*, *5*(12), 1348–1354.

Polymerdatabase. Flow properties of polymers. online: `http://polymerdatabase.com/polymer%20physics/Viscosity2.html`. Accessed: 2022-06-13.

Poon, C. (2022). Measuring the density and viscosity of culture media for optimized computational fluid dynamics analysis of in vitro devices. *Journal of the Mechanical Behavior of Biomedical Materials*, *126*, 105024.

Price, G. M., Wong, K. H., Truslow, J. G., Leung, A. D., Acharya, C., & Tien, J. (2010). Effect of mechanical factors on the function of engineered human blood microvessels in microfluidic collagen gels. *Biomaterials*, *31*(24), 6182–6189.

Pries, A. R., Neuhaus, D., & Gaehtgens, P. (1992). Blood viscosity in tube flow: dependence on diameter and hematocrit. *American Journal of Physiology-Heart and Circulatory Physiology*, *263*(6), H1770–H1778. PMID: 1481902.

Qin, D., Xia, Y., & Whitesides, G. M. (2010). Soft lithography for micro-and nanoscale patterning. *Nature protocols*, *5*(3), 491.

Raj M, K. & Chakraborty, S. (2020). Pdms microfluidics: A mini review. *Journal of Applied Polymer Science*, *137*(27), 48958.

Ramadan, Q. & Zourob, M. (2020). Organ-on-a-chip engineering: Toward bridging the gap between lab and industry. *Biomicrofluidics*, *14*(4), 041501.

Ren, X., Bachman, M., Sims, C., Li, G., & Allbritton, N. (2001). Electroosmotic properties of microfluidic channels composed of poly (dimethylsiloxane). *Journal of Chromatography B: Biomedical Sciences and Applications*, *762*(2), 117–125.

Rosen, L. A., Hollis, T. M., & Sharma, M. (1974). Alterations in bovine endothelial histidine decarboxylase activity following exposure to shearing stresses. *Experimental and Molecular Pathology*, *20*(3), 329–343.

Russo, T. A., Banuth, A. M., Nader, H. B., & Dreyfuss, J. L. (2020). Altered shear stress on endothelial cells leads to remodeling of extracellular matrix and induction of angiogenesis. *PLOS ONE*, *15*(11).

Sabanci University Information Center. 3D Printer. online: `https://www.sabanciuniv.edu/bm/tr/makerspace/hardware/3d-printer`. Accessed: 2022-06-15.

Sastry, S. K. & Horwitz, A. F. (1993). Integrin cytoplasmic domains: mediators of cytoskeletal linkages and extra-and intracellular initiated transmembrane signaling. *Current opinion in cell biology*, *5*(5), 819–831.

Schwartz, M. A., Schaller, M. D., & Ginsberg, M. H. (1995). Integrins: emerging paradigms of signal transduction. *Annual review of cell and developmental biology*, *11*, 549–599.

Secomb, T. W. (2016). Hemodynamics. *Comprehensive physiology*, *6*(2), 975.

Shigeo, A. (2000). Laminar shear stress inhibits vascular endothelial cell proliferation by inducing cyclin-dependent kinase inhibitor p21sdi/cip1/waf1. *Circ Res*, *86*, 185–190.

Sonmez, U. M., Cheng, Y.-W., Watkins, S. C., Roman, B. L., & Davidson, L. A. (2020). Endothelial cell polarization and orientation to flow in a novel microfluidic multimodal shear stress generator. *Lab Chip*, *20*, 4373–4390.

Souilhol, C., Serbanovic-Canic, J., Fragiadaki, M., Chico, T. J., Ridger, V., Roddie, H., & Evans, P. C. (2020). Endothelial responses to shear stress in atherosclerosis: a novel role for developmental genes. *Nature Reviews Cardiology*, *17*(1), 52–63.

Sui, G., Wang, J., Lee, C.-C., Lu, W., Lee, S. P., Leyton, J. V., Wu, A. M., & Tseng, H.-R. (2006). Solution-phase surface modification in intact poly (dimethyl-siloxane) microfluidic channels. *Analytical chemistry*, *78*(15), 5543–5551.

Tajeddin, A. & Mustafaoglu, N. (2021). Design and fabrication of organ-on-chips: promises and challenges. *Micromachines*, *12*(12), 1443.

Thompson, C. L., Fu, S., Heywood, H. K., Knight, M. M., & Thorpe, S. D. (2020). Mechanical stimulation: a crucial element of organ-on-chip models. *Frontiers in Bioengineering and Biotechnology*, *8*, 602646.

Thompson, D. & Bonner, J. (1992). *On Growth and Form*. Cambridge paperbacks. Cambridge University Press.

Trantidou, T., Elani, Y., Parsons, E., & Ces, O. (2017). Hydrophilic surface modification of pdms for droplet microfluidics using a simple, quick, and robust method via pva deposition. *Microsystems & nanoengineering*, *3*(1), 1–9.

Tsaryk, R., Yucel, N., Leonard, E. V., Diaz, N., Bondareva, O., Odenthal-Schnittler, M., Arany, Z., Vaquerizas, J. M., Schnittler, H., & Siekmann, A. F. (2022). Shear stress switches the association of endothelial enhancers from etv/ets to klf transcription factor binding sites. *Scientific reports*, *12*(1), 1–15.

Vasant, R. P., Appasaheb, P. S., Bhausaheb, D. S., & Sitaram, M. D. (2021). Review on organ on chip. *Asian Journal of Pharmacy and Technology*, *11*(1), 66–71.

Villegas, M., Cetinic, Z., Shakeri, A., & Didar, T. F. (2018). Fabricating smooth pdms microfluidic channels from low-resolution 3d printed molds using an omniphobic lubricant-infused coating. *Analytica chimica acta*, *1000*, 248–255.

Vining, K. H. & Mooney, D. J. (2017). Mechanical forces direct stem cell behaviour in development and regeneration. *Nature Reviews Molecular Cell Biology*, *18*(12), 728–742.

Vogel, V. & Sheetz, M. (2006). Local force and geometry sensing regulate cell functions. *Nature Reviews Molecular Cell Biology*, *7*(4), 265–275.

Walker, H. K., Hall, W. D., & Hurst, J. W. (1990). Clinical methods: the history,

physical, and laboratory examinations.

Wang, J. H.-C. & Thampatty, B. P. (2006). An introductory review of cell mechanobiology. *Biomechanics and modeling in mechanobiology*, *5*(1), 1–16.

Wautelet, M. (2001). Scaling laws in the macro-, micro-and nanoworlds. *European Journal of Physics*, *22*(6), 601.

Wevers, N. R., Kasi, D. G., Gray, T., Wilschut, K. J., Smith, B., van Vught, R., Shimizu, F., Sano, Y., Kanda, T., Marsh, G., et al. (2018). A perfused human blood–brain barrier on-a-chip for high-throughput assessment of barrier function and antibody transport. *Fluids and Barriers of the CNS*, *15*(1), 1–12.

Whitesides, G. M., Ostuni, E., Takayama, S., Jiang, X., Ingber, D. E., et al. (2001). Soft lithography in biology and biochemistry. *Annual review of biomedical engineering*, *3*(1), 335–373.

Winkler, T. E., Feil, M., Stronkman, E. F., Matthiesen, I., & Herland, A. (2020). Low-cost microphysiological systems: feasibility study of a tape-based barrier-on-chip for small intestine modeling. *Lab on a Chip*, *20*(7), 1212–1226.

Young, E. W. & Beebe, D. J. (2010). Fundamentals of microfluidic cell culture in controlled microenvironments. *Chemical Society Reviews*, *39*(3), 1036–1048.

Zhang, H. & Labouesse, M. (2012). Signalling through mechanical inputs–a coordinated process. *Journal of cell science*, *125*(13), 3039–3049.

Zhang, Y. (2020). *Multi-scale Extracellular Matrix Mechanics and Mechanobiology*. Springer.

Zhou, J., Ellis, A. V., & Voelcker, N. H. (2010). Recent developments in pdms surface modification for microfluidic devices. *Electrophoresis*, *31*(1), 2–16.

APPENDIX A

Microfabrication Protocol

This appendix covers the details of the work which was done to fabricate the employed chips. It consists of mold design, PDMS molding, and bonding.

Mold Design

Soft lithography has been selected to perform the fabrication since it is in accordance with the material, PDMS, which is soft and capable to be molded. The chip consists of two PDMS substrates and only a mold is required to transform the patterns for the top one. A simple petri dish is used to mold and fabricate the flat bottom substrate.

To design the following steps should be considered:

- Use Solidwork for easier modeling.

- First, the bed of the mold where the channels are on it needs to be designed with specific dimensions according to the chip size.

- **Point 1**: The thickness of the bed must be at least 5 mm to avoid bending the mold.

- **Point 2**: In bigger molds, it is required to add beams to cancel the bending as illustrated in figure A.1.
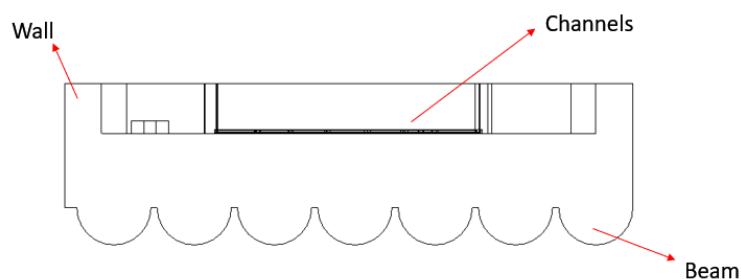

Figure A.1 Schematic of the bed thickness and beams of the mold.

- The next step is adding walls to the mold with a defined thickness (3 mm) which holds the PDMS inside the mold during the curing step.

Point: Add a fillet to the top walls for easy demolding and also as an indicator of the top side.

- On the upper surface of the bed, draw the considered patterns for the channel(s) having a defined width and length (trying the centerlines would help).

- Extrude the channels according to the designed height.

- All inlets and outlets need to be defined as pillars on the surface of the bed (Fig. A.2).
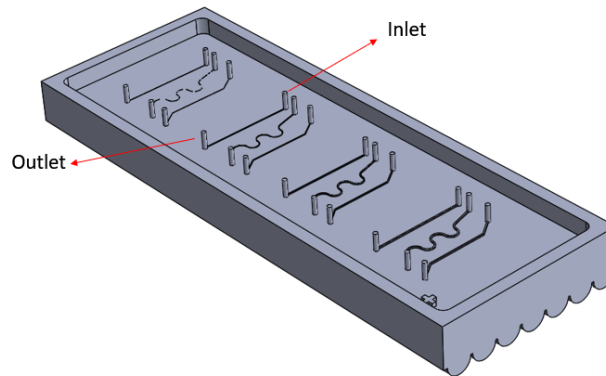

Figure A.2 Cad design of the molds; pillars are to open inlets and outlets

- To save the design and prepare it for 3D printing, the output format must be in ".stl" and in the options set the "Deviation" and "Angle" tolerance to its maximum amount (Fig. A.3).
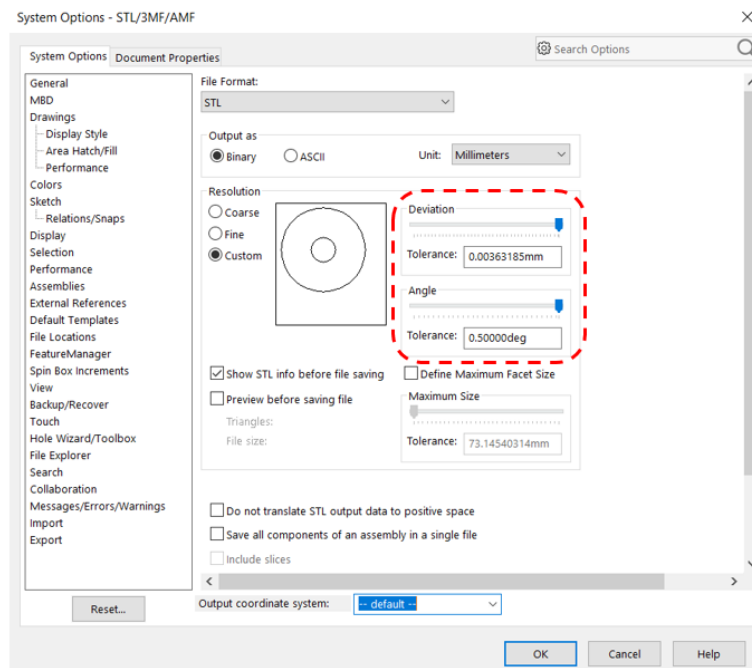

Figure A.3 Output format setup in SolidWork.

- The files can be printed with any high-resolution 3D printer.
- Use high-resolution photopolymer resin (GPBK04- Black resin- Formlabs.co) for better results.

Post printing treatment

- To make sure the resin has been cured completely and it is not sticky for pouring PDMS, put it in a UV and heat treatment chamber for 1 hour.
- The used resin is almost invulnerable to IPA, so it can be cleaned with IPA as well.

Pouring PDMS

- Polydimethylsiloxane (PDMS) (Sylgard 184 silicone elastomer kit, Dow Corning) has been used to fabricate microchannels.
- Prepare a sufficient amount of PDMS with the ratio of 10:1 (sylgard silicone elastomer base: Sylgard silicone elastomer curing agent).
- Mix for 5-10 minutes.
- Use a vacuum chamber for degassing.
- Pour into molds.
- Turn on the heater and set at 75°C.
- Wait for 3 to 4 hours.
- It is ready to take out of the oven and start demolding.

Demolding

- Use a blade to cut the bottom side of the substrate.
- Use a tweezer and detach it completely.
- Put scotch tape on the channel side to protect it from dust.

Bonding

- For bonding of the patterned substrate to the flat one, periodic infusion of oxygen is applied to activate the substrates (using a plasma chamber).
- Open O_2 gas for 10 mBar.
- Vacuum the tank to reach 200 mTorr.
- Rotate the valve to send O_2 inside and close it. Pressure will increase, wait to decrease.
- Open RF to "HIGH" level (29.6 W)when pressure is about 1200 mTorr.
- Wait for plasma emission to finish.
- Now the chamber is clean, vent the vacuum after turning off the RF and place your samples inside. Bonding faces should be upward.
- Start the vacuum.
- When the vacuum level decreased to 200 mTorr, open and close the valve quickly to insert oxygen and level up the pressure. - Wait for 1200 mTorr and turn on the RF with the "HIGH" level. When the pressure drops to 200 mTorr, turn off the RF ("OFF"). This is equivalent to 10 seconds of plasma treatment.
- Repeat the previous step three times.
- Turn the vacuum off and vent the chamber.
- Open the chamber and put the activated surfaces to each other and apply medium pressure.
- For stronger bonding, out inside a 60°C chamber for 3 minutes.